CLK8 reprograms rhythmic transcriptome and delay replicative senescence in MRC-5

by

Ufuk Can Solmaz

A Dissertation Submitted to the

Graduate School of Sciences and Engineering

in Partial Fulfilment of the Requirements for

the Degree of

Master of Science

in

Data Science

KOÇ
ÜNİVERSİTESİ

September 5, 2022

CLK8 reprograms rhythmic transcriptome and delay replicative senescence in MRC-5

Koç University

Graduate School of Sciences and Engineering

This is to certify that I have examined this copy of a master's thesis by

Ufuk Can Solmaz

and have found that it is complete and satisfactory in all respects,

and that any and all revisions required by the final

examining committee have been made.

Committee Members:

_____

Prof. İ.Halil Kavaklı

_____

Assoc. Prof. Atay Vural

_____

Prof. Nuri Öztürk

_____

Asst. Prof. Onur Öztaş

_____

Asst. Prof. Mehmet Tardu

Date: 08.09.2022

To my beloved parents Gülafer and Yusuf
and to my nephew Hakan Deniz Solmaz
for their endless support

ABSTRACT

The circadian clock is one of the time-keeping systems in organisms that regulate behavioral/or physiological changes with about 24-hour period. These rhythmic changes are generated by a transcriptional-translational regulatory feedback loops (TTFL) mechanism via core clock proteins at the molecular level. Simply, BMAL1 and CLOCK heterodimerize and activate the expression of E-box-containing genes such as PER2 and CRY1. The PER2:CRY1 complex along with Casein kinase Iε/δ translocates into the nucleus and represses their own expression. Almost 43% of gene coding genes are under the control of the circadian clock that is progressively disturbed with advancing age in terms of amplitude and period. Proper maintenance of the circadian clock is essential for homeostasis since the circadian clock is directly connected with vital systems such as reproduction, immunity and development.

Our group recently identified a small molecule, CLK8, that enhances circadian amplitude. To investigate the effect of CLK8 on ageing cells and on the robustness of the circadian clock in vitro, I regularly treated human lung fibroblast cells (MRC-5) with CLK8. I showed that CLK8 helps maintain the circadian clock of the aged cells and decreases cellular senescence by enhancing telomerase activity and maintain the telomeres. Furthermore, I have taken genome-wide approach to understand the effect of CLK8 using RNA sequencing. Analysis of the RNA-seq data revealed that CLK8 maintain oscillation of the genes, play key role in ageing. These results indicate that CLK8 shows great potential in the treatment of age-related diseases related with circadian clock.

ÖZETÇE

Sirkadiyen saat, yaklaşık 24 saatlik bir periyotta davranışsal/veya fizyolojik değişiklikleri düzenleyen organizmalardaki zaman tutma sistemlerinden biridir. Bu ritmik değişiklikler, moleküler düzeyde çekirdek saat proteinleri aracılığıyla bir transkripsiyonel-translasyonel düzenleyici geri besleme döngüleri (TTFL) mekanizması tarafından üretilir. Basitçe, BMAL1 ve CLOCK, PER2 ve CRY1 gibi E-box içeren genlerin ekspresyonunu heterodimerize eder ve aktive eder. PER2:CRY1 kompleksi, Kazein kinaz Iε/δ ile birlikte çekirdeğe yer değiştirir ve kendi ifadesini bastırır. Gen kodlayan genlerin yaklaşık %43'ü, genlik ve periyot açısından ilerleyen yaşla birlikte giderek bozulan sirkadiyen saatin kontrolü altındadır. Sirkadiyen saat, üreme, bağışıklık ve gelişme gibi hayati sistemlerle doğrudan bağlantılı olduğundan, homeostaz için sirkadiyen saatin uygun şekilde bakımı çok önemlidir.

Grubumuz kısa süre önce sirkadiyen genliği artıran küçük bir molekül olan CLK8'i tanımladı. CLK8'in yaşlanan hücreler üzerindeki etkisini ve in vitro sirkadiyen saatin sağlamlığı üzerindeki etkisini araştırmak için insan akciğer fibroblast hücrelerini (MRC-5) düzenli olarak CLK8 ile tedavi ettim. CLK8'in yaşlı hücrelerin sirkadiyen saatini korumaya yardımcı olduğunu ve telomeraz aktivitesini artırarak ve telomerleri koruyarak hücresel yaşlanmayı azalttığını gösterdim. Ayrıca, RNA dizilimi kullanarak CLK8'in etkisini anlamak için genom çapında bir yaklaşım benimsedim. RNA-seq verilerinin analizi, CLK8'in genlerin salınımını sürdürdüğünü ve yaşlanmada anahtar rol oynadığını ortaya çıkardı. Bu sonuçlar, CLK8'in sirkadiyen saat ile ilgili yaşa bağlı hastalıkların tedavisinde büyük potansiyel gösterdiğini göstermektedir.

ACKNOWLEDGEMENTS

First and foremost, I would like to express my special gratitude to my advisor, Prof. İ.Halil Kavaklı. He contributed to me much in science, philosophy, and scientific thinking. I think this thesis would not be possible without his immense guidance and support.

I want to thank my co-advisor, Assoc. Prof. Atay Vural for his assistance and counseling. I also appreciated my thesis committee members Prof. Nuri Öztürk, Asst. Prof. Onur Öztaş and Asst. Prof. Mehmet Tardu for their insightful comments and propositions.

I want to specially state my gratitude to Asst. Prof. Şeref Gül for illuminating and helping me with experimental and analysis perspectives. I will always remember his contributions to my life.

Starting from Seden Nadire Efenti, I am grateful to all HKLAB members. Working in this great team was a tremendous privilege. I also uniquely express my gratefulness to my assistant Göksu Türker. Throughout the thesis, she assisted me in various steps in both experimental and paper stuff. I will always miss and remember our cooperation and the charming environment we created with Seden Nadire Efenti, Göksu Türker, and Kamila Bazarbek. I hope we will accomplish colossal discoveries in science.

I thank Koç University and Koç University Hospital for their feasibility and financial support.

I am also lucky to have a great family who always supported me at the breaking points of my life. I want to praise my cousin Erdem Berk Kaya and my friend Tuğçe Gül for their mental and motivational support.

TABLE OF CONTENTS

LIST OF TABLES

LIST OF FIGURES

NOMENCLATURE

AMP: Adenosine monophosphate

AMPK: AMP-activated protein kinase

ATP: Adenosine triphosphate

ATR: Serine/threonine-protein kinase ATR

BMAL1: Aryl hydrocarbon receptor nuclear translocator-like protein 1

CDK2: Cyclin-dependent kinase 2

CK1 δ/ε: Casein kinase 1 epsilon/1 sigma

CLK8: 2-[2-(8,8-Dimethyl-2-oxo-4-phenyl-9,10-dihydropyrano[2,3-f]chromen-5- yl) oxyacetamido]benzamide

CLOCK: Circadian locomotor output cycles kaput

CRY: Cryptochrome

DBP: D site of albumin promoter (albumin D-box) binding protein

DKC1: Dyskerin Pseudouridine Synthase 1

DMSO: Dimethyl sulfoxide

E-box: Enhancer box

FBXLs: F-box/LRR-repeat proteins

GAR1: GAR1 Ribonucleoprotein

HIPK1: Homeodomain-interacting protein kinase 1

hTERT: Human telomerase reverse transcriptase

MEF: Mouse Embryonic Fibroblasts

MRAS: Ras-related protein M-Ras

NAMPT: Nicotinamide phosphoribosyltransferase

NES sequences: Nuclear export signal sequences

Nfil3: Nuclear factor, interleukin 3 regulated

NFKB1: Nuclear factor NF-kappa-B p105 subunit

NHP2: NHP2 Ribonucleoprotein

NLS: Nuclear localization sequence

NMDA: N-methyl-D-aspartic

NOP10: NOP10 Ribonucleoprotein

NRAS: GTPase NRas

PACAP: Pituitary adenylate cyclase-activating polypeptide

PER: Period

PTEN: Phosphatidylinositol 3,4,5-trisphosphate 3-phosphatase

PTMs: Post-translational modifications

RB1: E3 ubiquitin-protein ligase PPP1R1

REVERBs: Nuclear receptor subfamily 1, group D

ROREs: Retinoic acid-related orphan receptor response elements

ROS: Reactive oxygen species

SASPs: Senescence-associated secretory phenotype

SCN: Suprachiasmatic nucleus

SIRTs: Sirtuins

TERT: Telomerase reverse transcriptase

TGFBR2:TGF-beta receptor type-2

TERF1,TRF1: Telomeric repeat-binding factor I

TERF2,TRF2: Telomeric repeat-binding factor II

TRPM7: Transient receptor potential cation channel subfamily M member 7

TTFL:Transcription-translation feedback loops

β-TCP: β-tricalcium phosphate

CHAPTER 1

INTRODUCTION

Circadian rhythms are metabolic, biochemical, behavioral, and physical changes that follow 24 hours cycle. From cyanobacteria to mammals, circadian rhythms provide better fitness because of adaptation to environmental clues such as the light and dark cycle [3,4].

In mammals, the suprachiasmatic nucleus (SCN) and peripheral tissues generate these rhythms and synchronize the body with the surrounding environment via hormonal and neuronal pathways. At the molecular level, peripheral tissues and SCN generate circadian rhythms with interlocked transcriptional translational feedback loops (TTFLs). Primary TTFL is composed of a negative and positive arm [17]. The positive arm consists of circadian locomotor output cycles caput (CLOCK) and aryl hydrocarbon receptor nuclear translocator-like protein 1 (BMAL1), which heterodimerize and bind E-box sequences at the promoter of clock-controlled genes to activate gene expression. This heterodimer also initiated the expression of the period (PER) and cryptochrome (CRY). PER and CRY proteins create a negative arm via forming a heterodimer in the cytosol and translocating into the nucleus with casein kinase 1ε (CK1ε). This heterodimer complex represses the activity of CLOCK:BMAL1 driven transcription. After the degradation of PER and CRY, CLOCK:BMAL1 driven transcription re-starts. This feedback loop takes around 24 hours [22].

Approximately 43% of all coding genes in mice have cycling expression patterns under the circadian clock, which states the central role of the circadian clock in maintaining homeostasis [80]. Recent studies have revealed that malfunctioning of the mammalian circadian system is directly linked to various diseases such as sleep disorders, metabolic diseases, cardiovascular diseases, and aging. Moreover, circadian rhythms lose their robustness through cellular and organismal aging, and their amplitudes are damped. Hence, several groups have started identifying small molecules that target core clock components to treat circadian-related diseases and reveal

Replicative senescence is a cellular state in cells arrested and cannot proliferate further because of the lack of unique sequences called telomeres [55]. Telomerase activity extends telomere sequences at the end of chromosomes and provides chromosomal stability. However, rather than stem cells and germ cells, all cell types have restricted telomerase activity under the control of the circadian clock [59,60].

Recently, our group identified a small molecule, CLK8, that binds to CLOCK and disrupts the interaction between CLOCK and BMAL1. It reduces the amount of CLOCK in the nucleus and leads to enhanced circadian rhythm amplitude [24]. I treated lung fibroblast cells (MRC-5) with CLK8 to conserve the robustness of circadian rhythms in aging. I performed biochemical and transcriptomic to investigate the effects of CLK8 on aging. CLK8 treatment significantly increased telomere length and telomerase activity in vitro and decreased the number of cells that entered the cellular senescence. Furthermore, compared to the control group, a number of cyclic genes have a ~2-fold increase in CLK8 that states circadian control has enhanced with CLK8 treatment in aging. The use of CLK8 would both improve age-related conditions and age-related decline of the circadian clock.

Chapter 2 provides literature review about molecular mechanism of mammalian circadian rhythms and its relationship with cellular senescence.

Chapter 3 explains related material methods employed in this thesis.

Chapter 4 shows the results obtained during this study.

Chapter 5 discusses outcomes of this thesis.

CHAPTER 2

LITERATURE REVIEW

2.1. Biological Rhythms

Almost all organisms have to detect environmental clues for both synchronization and adaptation that have led to biological rhythms throughout the history of evolution. Understanding the cycling changes in the environment like seasons, weeks, and days increases organisms' fitness [1,2]. As a consequence of this advantage, different cycling metabolic processes have evolved in species from unicellular to multicellular organisms [3]. These biological rhythms have been classified into three groups according to the length of their periods. The first group is composed of infradian rhythms that have periods greater than 24 hours, such as hibernation and skin change in some animals. That is followed by circadian rhythms that extend around 24 hours and are related to daily rhythms such as hormonal, metabolic controls, and sleep-wake cycles. Third biological rhythms are ultradian rhythms that include cycling events that take less than 24 hours, such as blinking, feeding, and blood circulation [4-7].

2.2. Circadian Rhythms

Circadian rhythms are 24 hours periodical changes in metabolism, physiology, and behavior that have been conserved from cyanobacteria to human beings. As cycling of abiotic events, organisms adapt their metabolism accordingly. For example, nitrogen fixation and photosynthesis metabolism have tightly regulated under the circadian clock in cyanobacteria. Under the control of the circadian clock, cyanobacteria favor photosynthesis or nitrogen fixation concerning the availability of sunlight and oxygen [3]. Moreover, several knockout studies have shown that abolishing or disrupting the circadian clock in cyanobacteria significantly decreases the organism's fitness and provides the survival advantage of having a circadian clock throughout evolution [8].

The animal kingdom also has circadian clocks that regulate their activity and homeostasis. Metabolism of both nocturnal and diurnal animals have hierarchically

controlled by circadian clocks, which determine their hunting, activity, and feeding behaviors. Mice have abolished clocks show irregular feeding and activity patterns followed by metabolic non-functionalities and increased disease- susceptibility [9,10].

Even though various rhythms in nature follow ~24 hours periodicity, not all of them are circadian rhythms. A rhythm must satisfy three main properties in order to be circadian. Initially, it should be intrinsic and free running [11,12,14]. Even in the absence of environmental clues, it must persist. For example, in *Mus musculus* or *Drosophila melanogaster,* circadian rhythms persist in constant dark or light conditions [13,15]. Furthermore, it should compensate for the temperature changes in biological levels without being affected. Lastly, circadian rhythms must be entrainable depending on nonexperimental clues. Feeding, exercise, and light exposure are well-established entrainers [11-14].

2.3. Mammalian Circadian Clocks

Mammalian circadian clocks are organized hierarchically and composed of various oscillations in cellular, tissue, and system levels. The suprachiasmatic nucleus (SCN) is located in the hypothalamus and roughly consists of 20.000 neurons and serves as a master clock/peacemaker [16]. Blue light is received by retinal ganglion cells, and it is transmitted to SCN via the retinohypothalamic tract. SCN resets cellular oscillation by inducing *Per 1,* whose expression is enhanced by N-methyl-D-aspartic (NMDA) glutamatergic and pituitary adenylate cyclase-activating polypeptide (PACAP) signaling pathways [18,19]. SCN synchronizes other peripheral clocks via both hormonal and neuronal pathways [20]. Even though this synchronization, recent findings have also revealed the independence of peripheral clocks. For instance, the liver has a clock that can synchronize itself by feeding habits independent from the peacemaker [21].

2.4. Molecular Architecture of Mammalian Circadian Clocks

Circadian oscillations are composed of loops controlled in both transcription and transcriptional manner. These interlocked transcription-translation feedback loops (TTFL) are the primary control mechanism of circadian rhythms in mammals. There are three main

TTFLs that maintain oscillations in mammals. Prominent and most studied TTFL is composed of 4 different proteins and their isoforms which are BMAL1, CLOCK, PER2, and CRY1. First, TTFL begins with heterodimerization of transcription activator CLOCK and BMAL1 in the cytosol. This heterodimer shuttles the nucleus and target enhancer sequences of genes with E-box motifs. These activators are referred to as the positive arm of the TTFL. This heterodimer also targets Period (Per1, Per2, Per3) and Cryptochrome (Cry1, Cry2) genes that will create the negative arm of the loop [17,22,24]. Per1 and Cry2 accumulate in cytosol over time, and finally, they form a heterodimer. This Per: Cry2 complex interact with casein kinase I isoforms (CK1 ε/δ) and translocate in the nucleus, where they repress their own transcription with inhibition of Clock: Bmal1 complex [23]. This repression event is followed by the degradation of the Per2:Cry1 complex via the ubiquitin-proteasomal pathway. Even though the degradation of the Per: Cry1 complex is well understood, the degradation of CLOCK:BMAL1 or Bmal1 in the nucleus has not been illuminated clearly [25,26].

The second feedback loop targets the regulation of ROREs (retinoic acid-related orphan receptor response elements), including promoters. Primarily, the expression of Bmal1 and Nfil3 is tightly controlled. Regulation of expression of ROREs, including promoters activated and repressed by RORs and REVERBs [27].

The expression of DBP is also E-box regulated. In the last feedback loop, DBP and NFIL3 work antagonistically similar to ROR and REVERBs to regulate the expression of D-box-containing promoters. In contrast to RORs promoter, REVERBs include E-box elements. Therefore, that makes dual control of the expression of REVERBs by CLOCK: BMAL1 and DBP/NFIL3[17,27].

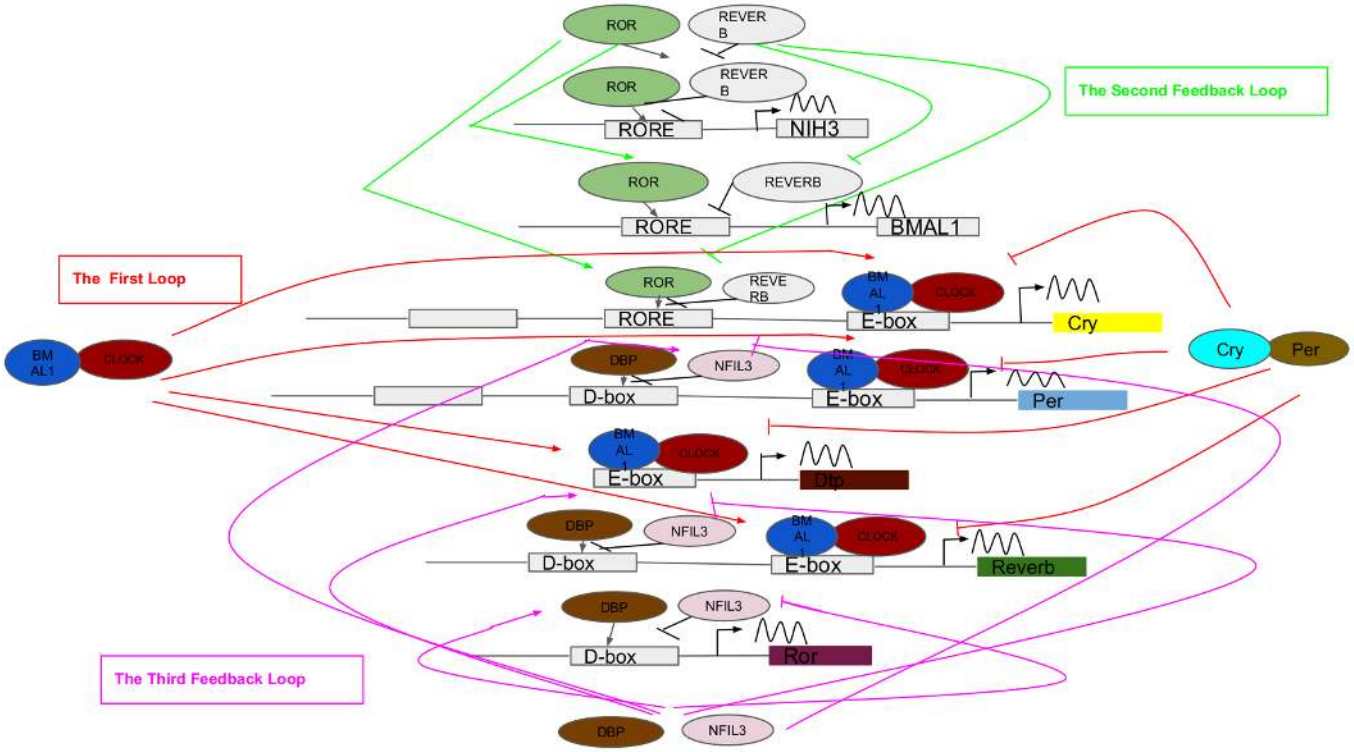

Figure 2.1 Three intervened TTFLs of mammalian circadian clock. Adapted from [23].

These interlocked loops lead to the occurrence of cyclic expression of genes. E-boxes, D-boxes, and ROREs are regulating the phase of gene expressions. D-boxes are active during the day, ROREs take a role in the evening, and E-boxes control the expression of genes in the morning [17,27].

In regulating these TTFLs, three central controlling systems are post-translational modifications (PTMs), translocation, and turnover rates. Phosphorylation is one of the primary modifications affecting the stability and entrance of core clock proteins such as PERs. For example, phosphorylation of PERs by casein kinase 1δ and 1ε leads to ubiquitinylation by β-transducin repeat-containing protein (β-TCP) [17,29]. On the other hand, CK1-mediated phosphorylation is necessary for the nuclear entry of PERs. These phosphorylation-dependent control mechanisms occur in different regions of PERs; therefore, the phosphorylation site is also a determining factor for the future of proteins [30,31].

On the other hand, acetylation of PERs increases stability, and O-GlcNAcylation decreases stability and accelerates repression [31].

There are differences in the repression activity of CRYs and PERs on CLOCK: BMAL1.CRYs display higher repression activity than PERs [17,23,32]. However, CRYs stability is directly affected by the phosphorylation and ubiquitination of PERs; even CRYs can exhibit repression activity in the absence of PERs since it has been hypothesized that there is a kind of competition between FBXL3 and PERs for binding the CRYs in the nucleus [33]. Like differential phosphorylation sites of PERs, CRYs have differential ubiquitination sites that can interact with FBXL proteins. Subcellular localization and interactions with different FBXL proteins affect the stability and fate of CRYs. FBXL3 is one of the main E3 ubiquitin ligases that regulate the stability of CRYs by poly-ubiquitination in the nucleus with SKP1-CUL1-F-box protein. However, ubiquitination of CRYs in the nucleus by FBXL21 interferes with the binding of FBXL3 and stabilizes CRYs. In contrast, if this ubiquitination takes place in the cytosol, it promotes degradation [23,33,34].

2.5. Relation Between Stoichiometry of Clock Proteins and Circadian Rhythms

Initially, CLOCK lacks nuclear localization and nuclear export signals (NLS, NES) that prevent it from entering the nucleus independently from BMAL1. Therefore, the positive arm of the clock is present as CLOCK: BMAL1 heterodimer in the nucleus. In the negative arm, even though both PERs and CRYs have both NLS and NES sequences, the entrance of PERs into the nucleus depends on CRYs interactions [35].

When the abundance of core clock proteins was investigated, gel-filtration chromatography assays in mice revealed that CLOCK: BMAL1 is much more abundant than PER: CRY. In vitro studies with MEF (Mouse Embryonic Fibroblasts) show no significant differences between the abundance of CRY1 and positive arm proteins in the nucleus, but for the case of PER2, it was almost half [36].

Maintenance of the stoichiometric ratio between positive and negative arms of clock proteins is crucial to conserving robust circadian rhythms at the molecular level. Knock out, knockdown, and overexpression studies demonstrate that strengthening or weakening the

arms of the circadian oscillator leads to the occurrence of different rhythm phenotypes [24,38]. For instance, overexpression of both CLOCK and BMAL1 leads to amplitude dampening in circadian rhythm with the elevation of mRNA levels of E-box controlled genes. This phenotype would arise from decreased repression activity of the negative arm. Other studies also revealed that silencing BMAL1 with siRNA or overexpression of PER2 leads to enhanced circadian amplitude in MEFs and *Bmal:dLuc* U2OS cells. These studies suggest that alterations in the stoichiometry of core clock proteins directly affect the amplitude of circadian rhythms [36-40].

2.6. CLK8 and Other Small-molecule Modifiers of Circadian Clock

The approach of small-molecule identification has arisen in the last two decades to reveal the mechanisms behind controlling circadian rhythms and creating therapeutics against circadian-related diseases. Two main methods for this purpose are high-throughput screening and structure-based studies [41]. Even though both techniques have disadvantages/advantages, they classify various molecules that directly interact with core clock components and lead to differentiation in the phenotype of circadian rhythms [41,42]. They are categorized according to their isoform specificity and amplitude, period, and phase effect.

Table 2.1 Several small molecules modifiers of circadian rhythms. Adapted from [42].

Name	Target Molecule/effect	Circadian Phenotype	Reference
CLK8	CLOCK	Amplitude enhancer	[24]
KL001	CRY stabilizer	Period lengthening	[68]
Nobiletin	ROR agonist	Enhancing amplitude and lengthening period	[69]
M47	CRY1 destabilizer	Period lengthening	[70]
KL201	CRY1 stabilizer	Period lengthening	[71]
GO044	CRY stabilizer	Period shortening	[72]

Our previous study demonstrated that CLOCK-specific small molecule CLK8 decreases the nuclear accumulation of CLOCK by disrupting the interaction between CLOCK and BMAL1. This effect leads to enhanced amplitude in circadian rhythms of

Bmal:dLuc U2OS, *Bmal:dLuc* NIH 3T3, and MDA MB231 cells in a dose-dependent manner. Additionally, rhythms got more robust. mRNA studies reveal the reduction in the expression of E-box controlled genes in mice [24].

2.7. Aging and Cellular Senescence

Aging is pneumonia, defined as deterioration in both functional and physical operations in a time-dependent manner that affects reproduction and survival of the organism. There are still debates about whether the progression of aging is programmed or not. From molecular to organism level, aging is directly related to abnormalities in regulation and control that lead to increased susceptibility to cancer, diseases, and death [43].

Environmental and genetic factors determine the life span. Various studies have revealed the positive effects of calorie restriction and exercise on life expectancy in the last century. Moreover, external factors like pollution, radiation, and high-fat food consumption have started to show their importance, and various studies have confirmed their effects on health and life span. Even though aging outcomes are easy to observe, how these alterations occur in a time-dependent manner remains unknown. Studies on the different model organisms revealed that decreased biological waste production, timed feeding, and activity enhanced the expected life span [44-46].

Senescence is an equivalent of aging in cellular level. It can be affected by both external and internal clues like organismal aging [47]. Cellular senescence or replicative senescence take place in somatic cells that lead irreversible growth arrest. Various factors can lead the cell arrest as an external factor such as lack of supplementation, toxicity, available area [48,49]. Those external factors have been well studied in vitro with various agents that mimics environmental stress such as 5-azacytidine and sodium butyrate [50].

2.8. Replicative Senescence, Telomeres and Telomerase

On the other hand, in prior studies that investigate the cultured cells, Hayflick realized that there is limited potential of dividing of cells [52]. This limitation was referred as Hayflick

limit and the processed was named as cellular senescence in the beginning. Following studies have identified the telomere dependency of this limitation of mortal cells and identified as replicative senescence. Even though Hayflick observed senescence in human diploid fibroblasts, other cell types like smooth muscle cells, glial cells, endothelial cells and T lymphocytes undergoes cellular senescence [51].

Five primary mechanisms trigger the cell either go in apoptosis or senescence-related stages. Those are related to oncogenes, replicative stress, reactive oxygen species (ROS) production, DNA damage, and dysfunctional telomerase activity. [53,54] In the replicative senescence perspective, two main mechanisms regulate telomere length. One is the integrity of telomeres, and the other is telomerase activity [55]. Several studies reveal that telomeric repeat binding factor 1 (TRF1) levels are decreasing with age in vitro, and overexpression of TRF1 reduces the DNA damage at telomere sequences, consequently, lead decreased senescence and prolonging mouse health span [56].

Telomere sequences play essential roles in regulating chromosomal stability and genomic integrity. It is composed of repetitive TTAGGG sequences, which create a shelterin complex with six different proteins. These subunits of the shelterin complex provide the DNA binding and recruitment of telomerase for elongation [57].

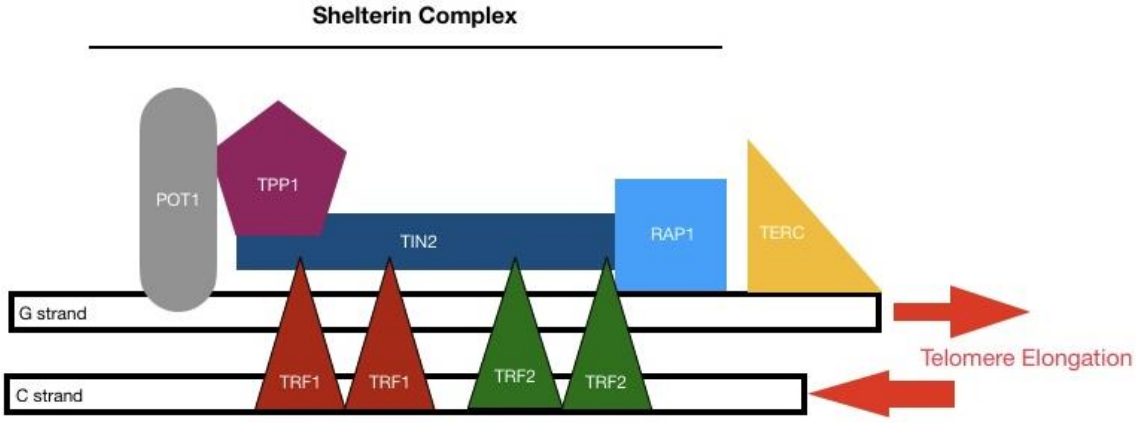

Figure 2.2. Structure of human telomere. Shelterin complex consist of six different proteins that bind telomeric DNA. Adapted from [55].

Furthermore, human telomerase reverse transcriptase (hTERT) is a holoenzyme that directly regulates the length of telomeric repeats. Even though its activity is directly affected

and controlled by mutations and tissue type, it is composed of RNA components TERTC, dyskerin (DKC1), NOP10, GAR1, and NHP2. hTERT uses RNA components as a template to catalytically add TTAGGG hexameric nucleotide repeats [55]. One recent study reveals that overexpression of hTERT subunit DKC1 leads to enhanced telomerase activity and lengthening telomere repeats in erythroleukemia cells [56,58]. Therefore, expression levels of different components of the hTERT complex would significantly impact replicative senescence.

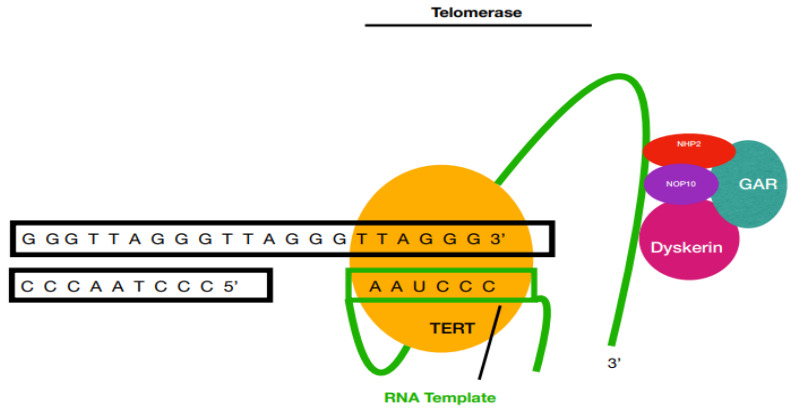

Figure 2.3. Structure and components of hTERT holoenzyme. Adapted from [57].

2.9. MRC-5 Cell Line

MRC-5 cells are lung fibroblast cells derived from the Caucasian male fetus and have approximately 42-46 doublings. When young cells are cultured, their doubling time takes around 36 hours. While aging, this time would increase up to 72 hours. One of the leading properties of MRC-5 is telomere shortening in time and entering cell cycle arrest, which can be easily detectable under the microscope via tracking enhanced cellular volume [73,74,75]. They started to prefer glycolysis over oxidative phosphorylation and enhance their beta-galactosidase activity through aging and replicative stress.

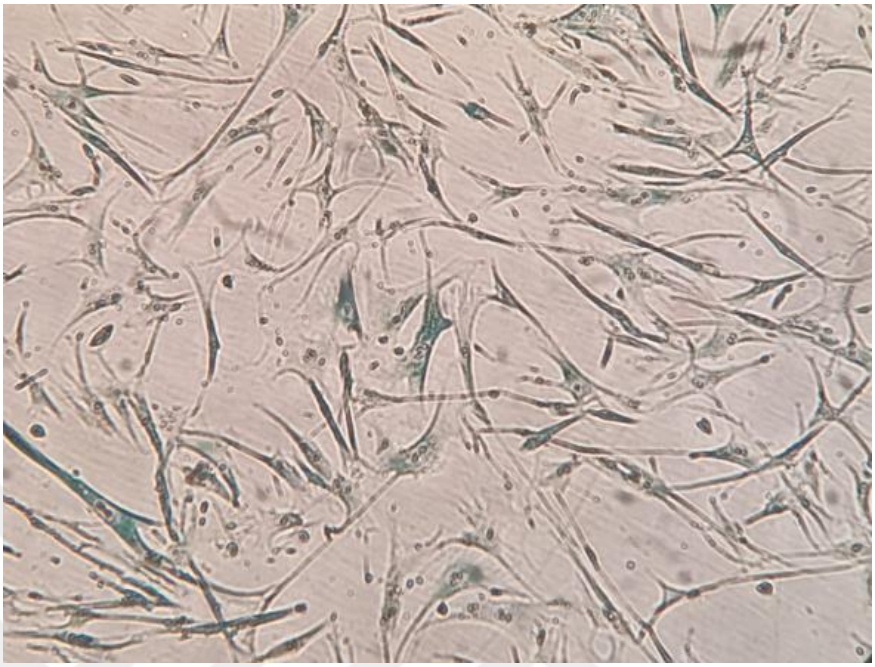

Figure 2.5. MRC-5 cells. Lung Fibroblast cells enters in replicative senescence in time and stained with X-gal.

2.10. Relationship Between Circadian Rhythms and Cellular Senescence

Recent studies have revealed that SCN has a delayed phase, damped amplitude, and lengthened period in aged mice [59,60]. Aged lung fibroblasts also show similar patterns in vitro [61]. Moreover, differences in circadian outputs in age are also tissue-dependent [62,82]. Molecular mechanisms of how aging affects the cellular clock remain unclear, but various pathways impaired in senescent cells are directly related to the circadian clock.

SIRTs are NAD^+-dependent deacetylases and interact with core clock components. For instance, rhythmically, SIRT1 and SIRT6 deacetylated histone H3 on a promoter on core clock genes. Therefore, NAD^+ levels should be carefully controlled. NAMPT is the rate-limiting enzyme in the NAD-Salvage pathway and shows a cycling pattern [64]. However, decreased NAD^+ levels are seen in cellular senescence and directly affect the expression of core clock genes. At this point, NAD^+ production is interlocked with the circadian clock, and

both are downregulated with age. Furthermore, rather than stoichiometry of NAD^+, its redox state would also influence the binding potential of NAPS2:BMAL1 to DNA [62-65].

AMPK is also rhythmically expressed kinases that alter the circadian clock through phosphorylation of CK1ε. Increased AMP/ATP ratio in aging would lead to an increased effect of AMPK on the circadian clock [66].

Polyamines regulate the interaction between CRY1 and PER2, and studies revealed that increased polyamines in aging mice lead to a lengthening period (ref-polyamine). Senescence-associated secretory phenotype (SAPS) is composed of more than 300 factors, some of which alter circadian phenotype [66,67].

Although abnormalities in the circadian clock in cellular senescence are not fully understood, these lines of evidence suggest that there are highly locked. Since cellular senescence related molecules mentioned above are also related with the circadian clock, dysfunction of the clock through time would lead to or enhance the cellular senescence profile.

CHAPTER 3

MATERIALS AND METHODS

3.1. Cell Culture

Human Lung Fibroblasts (MRC5) were used in all experimental setups as the primary source. Cells were maintained in the incubator at 37°C degrees under 5% CO2 and %95 humidity conditions for all experiments. Growth medium composed of Dulbecco's Modified Eagle Medium with high glucose and 2mM L-Glutamine (DMEM, Thermo Fisher Scientific), 10 % Fetal Bovine Serum (Thermo Scientific), 100ug/ml Penicillin/Streptomycin and 1% Non-Essential Amino Acids (NEAA, Thermo Scientific). Subculturing was performed when cells reached 85-90 % confluency. After removal of old media, cells were gently washed with 1X PBS solution and detached from the surface with 1ml Trypsin-EDTA (Multicell, Cat. No 325-043-EL). After 30-60 seconds, trypsin was inactivated with D10-NEAA medium, and cells were transferred to 15 ml falcons. The number of cells counted in the hemocytometer includes 10uL of the cell-containing media and split into new 90mm dishes with a 1:2 split ratio. Date, time, and the number of cells were noted to construct the growth curve. Both CLK8 and DMSO dissolved in DMEM. On the day following subculturing, cells were treated with either DMSO or CLK8, with the final concentration of CLK8 as 10 µM. MRC-5 cells were continuously treated with either DMSO or CLK8 from Population Doubling Number (PDL) 54 to 67.

3.2. Cell Cytotoxicity Assay

MTT (3-(4,5-dimethylthiazol-2-yl)-2,5-diphenyltetrazolium bromide) assay was performed to assess the cell viability in the presence of CLK8.5000 cells/well were seeded in a 96-well plate with D10-NEAA media and incubated for 48 hours in an incubator. Different dosages of CLK8 and DMSO were prepared in DMEM, and cells were treated accordingly. Cells have grown for another 48 hours. At the 96th hour the medium of cells was replaced with an MTT-DMEM medium (final concentration:1mg/ml). Cells were

incubated in an incubator for 4 hours, and their mediums were replaced with 200uL of DMSO-EtOH solution (1:1 vol) to dissolve formazan salts whose absorbance was detected in Synergy H1 Microplate Reader (Bio-Tek Instruments) in 600 and 690 nm respectively. Cell viability reference to DMSO was calculated as in **Equation 3.1.**

$$\%\ Cell\ Viablity = \frac{(A600nm - A690nm)SAMPLE}{(A600nm - A690nm)DMSO} \times 100$$

Equation 3.1. Cell viability calculation.

3.3. Beta-galactosidase Assay

On the first day, 30000 cells were seeded in a 24-well plate, and the following day, they were treated with either DMSO or 10µM CLK8. After 24 hours of drug treatment, cells were washed with cold 1X PBS twice. Cells were fixed on the surface of a 24-well plate with a fixation solution composed of 2% formaldehyde (vol/vol) and 0.2% glutaraldehyde and 1X PBS as a solvent. Samples were washed with 1X PBS twice after 5 minutes of fixation incubation. Each well incubated with 200uL of staining solution that includes 40mM citric acid/Na phosphate buffer, 5mM K_4[Fe $(CN)_6$], 5mM K_3[Fe $(CN)_6$], 150mM NaCl, 2mM MgCl2 and 1 mg/ml X-gal (BioFroxx,1168GR001) for overnight at 37°C in CO2-free incubator [110]. After incubation, cells were washed with 1X PBS twice and once with methanol. Finally, cells were counted under a bright-field microscope in 10X and 20X ocular.

3.4. Lentivirus Production

Young Hek293T (Passage:10) cells with 70-80% confluency were co-transfected with 10µg pLV6-Bmal1-dluc, µg pCMV-VSVG envelope, and 9µg pCMV-ΔR8.2dvpr (**Figure E.1**) packaging vectors with PEI as a transfection reagent in DMEM. After 16 hours of incubation at 37°C under 5% CO2, 3 ml of D10 medium was added. 48 and 72 hours after the transfection, cells were harvested and filtered in 0.45µm syringe filters (AISIMO, 210828). It has been aliquoted in 1.5ml Eppendorf's and has been stored in -80°C for long-term usage.

3.5. Lentivirus Transduction and Real-time monitoring of Circadian Oscillation

$2x10^5$ MRC-5 cells were seeded in 35 mm dishes in D10-NEAA medium, and the following day, the medium was replaced with lentivirus-containing media (750uL of lentiviral particles, 250uL DMEM,1ul of 8mg/ml protamine sulfate). After 72 hours of lentiviral transduction, cells were synchronized with two hours of 0.1μM dexamethasone incubation. Following to that media was replaced with LumiCycle media that consisted of 10g of low glucose DMEM powder supplemented with L-glutamine(Sigma D2902), 0.35 mg/ml sodium bicarbonate(Sigma S5761), 5% FBS(Gibco,16000044), %1 NEAA (Multicell 321-011-EL), 3.5 mg/ml D-(+)-glucose powder(Sigma G7021), 25U/mL streptomycin-penicillin(Gibco 15140-122), 10mM HEPES (Gibco 15630106) and an appropriate amount of either CLK8 or DMSO (10μM and 0.5vol/vol in final). The medium was enriched with 0.1mM Luciferin. After the media replacement, dishes were immediately sealed with silicone grease and kept out of the light as much as possible. In the final, dishes were placed into a LumiCycle luminometer (Actimetrics), and 5 days of bioluminescence were continuously recorded. LumiCycle Analysis software (Actimetrics) and BioDare2 [76] were used to quantify the circadian rhythm.

3.6. Subcellular Fractionation and Western Blotting

Stoichiometric changes between cytosol and nucleus have been investigated to confirm the effect of CLK8 on the same mechanism as our group proposed [24]. $4,5x10^5$ cells were seeded in a 90mm well plate, and 24 hours later, cells were treated with either 10μM CLK8 or DMSO. 48 hours after the seeding, cells were washed with 1X PBS and trypsinized. After inactivating trypsin with D10, cells were harvested and centrifuged at 5000g for 5 minutes at 4°C. Supernatants discarded and pellets resuspended with 60uL of Cytosolic Lysis Buffer (CLB; 10mM KCl, 0.05% NP-40, 0.1mM EDTA pH 8.0, 10mM HEPES pH 7.9, 1X PIC). After 10 minutes of incubation in the ice, samples were centrifuged at 3000rpm for 5 minutes, and supernatants were transferred into new 1.5ml Eppendorf's as cytosolic fragments. The same resuspension and centrifugation were performed again for the remaining pellet. Supernatants after the centrifugation were

discarded, and pellets were resuspended with 30uL of Nuclear Lysis Buffer (NLS;0.4M NaCl, 1mM EDTA, 10%Glycerol, 20mM HEPES pH 7.9, 1X PIC) and samples were sonicated for 2 times with BANDELIN SONOPULS HD 2070 Homogenizer (60% power, 3 cycles,10 seconds). After sonication, cytosolic and nuclear fractions were centrifuged at 15.000g for 10 minutes, and supernatants were collected. Protein concentrations were measured with Pierce 660nm Protein Assay. Subcellular fractions were denatured via addition of 4X Laemmli buffer (250mMTris-HCl pH 6.8, %40 Glycerol, %4 Sodium Dodecyl Sulfate (SDS), 0.02% Bromophenol Blue, %10 Beta-mercaptoethanol) and incubation at 95°C for 7 minutes.

30µM of samples were loaded into acrylamide gel that consist of %5 Stacking (1.5ml H2O,0.33ml %30 Acrylamide, 0.25ml 1M Tris-HCl Ph 8.8, 0.02ml 10% SDS, 0.02ml %10 ammonium persulfate,0.002ml TEMED)and %10 Separation (1.9ml H2O,1.7ml %30 Acrylamide, 1.3ml 1.5M Tris-HCl Ph 8.8, 0.05ml 10% SDS, 0.05ml %10 ammonium persulfate,0.002ml TEMED) gel. For immunodetection, anti-CLOCK (Bethyl, A302-618A), anti-BMAL1(Santa Cruz Biotech., SC-365645), anti-Histone H3(Abcam, ab1791), anti-αTUBULIN (Sigma-Aldrich, T9026) antibodies used. αTubulin and Histone H3 were performed for cytosolic and nuclear protein normalization.

3.7. Genomic DNA Isolation

2 x 10^5 cells were harvested and washed with 1X PBS. After centrifugation at 5000g for 7 minutes at 4°C, pellets were lysed with lysis buffer and genomic DNA (gDNA) was isolated with column binding with Monarch Genomic DNA Purification Kit (New England Biolabs, T3010S) according to product's manual.

3.8. Telomere Length Quantification

Telomere length of treated and control samples was quantified with a qPCR kit (Sciencell,8918). Telomere sequences were amplified for 5ng of gDNA and 1uL of the

reference genome. Telomere lengths of samples were determined with respect to the reference genome and single copy reference (SCR).

Table 2.1 qPCR conditions for telomere length quantification (Sciencell,8918).

Step	Temperature	Time	Number of Cycles
Initial denaturation	95°C	10min	1
Denaturation	95°C	20 sec	
Annealing	52°C	20 sec	
Extension	72°C	45 sec	32

The comparative quantification cycle value method has been used in determining telomere length as in **Equation 3.2**.

$$\Delta Cq\ (TEL) = Cq\ (TEL, target\ sample) - Cq\ (TEL, reference\ sample)$$

$$\Delta Cq\ (SCR) = Cq\ (SCR, target\ sample) - Cq\ (SCR, reference\ sample)$$

$$\Delta\Delta Cq = \Delta Cq\ (TEL) - \Delta Cq\ (SCR)$$

$$\text{Reference telomere length} \times 2^{-\Delta\Delta Cq}$$

$$\text{The total telomere length of cell (2n)} = \text{Reference telomere length } (708 \pm 52\ kb) \times 2^{-\Delta\Delta Cq}$$

Equation 3.2. Telomere length quantification.

3.9. Telomerase Activity Assay

Telomeric Repeat Amplification Protocol (TRAP) was performed with 2×10^5 cells which were harvested and washed with 1X PBS at 3000g for 5 minutes at 4°C (Roche,12013789001). Extract preparation was followed by PCR elongation/amplification, hybridization, and photometric detection. A control template that contains 0.001 amol/uL DNA template is preferred since the low activity of telomerase in MRC-5 cells.

3.10. Time Dependent RNA Isolation, cDNA Synthesis and RT-qPCR

1 x 10^5 cells were seeded in 12-well plates, and after the attachment of cells, they were either treated with DMSO or CLK8 (final concentration:10µM). When cells reached %75 confluences, mediums were replaced with 0.1µM dexamethasone/DMEM solution and were incubated for 2 hours. Following this, cells were treated with DMSO or CLK8. Cells were harvested from ZT0 to ZT42 with 6 hours intervals. Through harvesting, samples were washed with 1X PBS, and pellets were obtained after centrifugation at 5000g for 5 minutes at 4°C and finally stored at -80°C.

Samples were lysed, and total time-dependent RNA was bound to the column (Qiagen, 74106). After DNAse digestion, samples were isolated and stored at -80°C for long-term usage. The integrity, quality, and quantity of total RNA were investigated with Nanodrop 2000 (Thermo Scientific) and agarose gel electrophoresis (1% agarose gel in diethylpyrocarbonate-water and 1X Tris-Acetic acid-EDTA, 90Volt for 15 minutes).

cDNA was synthesized by Thermo Scientific's RevertAid First Strand cDNA Synthesis Kit. As described in product manual, each reaction composed of 5µM Oligo(dT)18 primer, 1X Reaction Buffer, 0.5ug RNA template, 1U/µL RiboLock RNase Inhibitor, 10U/µL RevertAid M-MuLV RT and 1mM dNTP mix. cDNAs were diluted 1:40 fold with Rnase-Dnase free water for qPCR reaction.

For each sample, the qPCR reaction consists of 10µL 2X SensiFAST SYBR ® No-ROX Mix (Bioline),6µL nuclease-free water, 3uL of diluted cDNA, and 1uL forward-reverse primer mix (0.5µM final concentration for each primer). The entire list of primers is given in **Table B1**. qPCR reaction was performed via the CFX Connect Real-Time PCR detection system (Bio-Rad). In the qPCR protocol, samples were initially denatured at 95°C for 7 minutes. Amplification was performed for 40 repeats composed of incubation at 95°C for 8 seconds, at 60°C for 20 seconds, and at 72°C for 20 seconds. After amplification, samples were incubated at 95°C for 8 seconds, at 70°C for 5 seconds, and 90°C for 5 seconds. The fluorescence signal was recorded throughout the PCR reaction. Products were analyzed by melting quantities and agarose gel electrophoresis (2% agarose gel in 1X Tris-Acetic acid-EDTA, 90Volt for 15 minutes). Ribosomal protein, large, P0(RPL0) used as a housekeeping gene, and expression of other genes

normalized accordingly. Data was generated according to $2^{-\Delta\Delta Ct}$ method.

3.11. RNA-seq Library Preparation and NGS analysis

Libraries were prepared for samples from ZT0 to ZT24, with three replicates. Total RNA samples were selected with Poly(a) mRNA magnetic beads (NEB, E7490) and isolated with NEBNextTM UltraTM II RNA Library Prep Kit for ILLUMİNA (#E7770; New England Biolabs). mRNA libraries size was adjusted to 300bp via incubation at 94°C for 15 minutes. Length and quantity of prepared libraries determined in agarose gel electrophoresis (1% agarose gel in 1X Tris-Acetic acid-EDTA, 90Volt for 15 minutes) and Qubit 2.0 Fluorometer (Invitrogen). Samples were sequenced. Sequencing was performed with the HSX platform.

Raw fastq data's quantity was checked with MultiQC (**Table 4.1**) and trimmed with Trimmomatic-0.39. After that, raw data aligned to the GRCh38 with STAR v2.5. Transcripts were quantified with RSEM v1.3.0 [78]. Transcripts per million values for all remaining libraries were merged into two expression tables as vehicle and treatment. Quantile normalization was performed with the R.3.5 preprocessor package. The rhythmicity of transcripts was determined with MetaCycle [79] meta2d function. Transcript base expression greater than 0.5 and p-values lower than 0.05 were assigned as rhythmic. Specific rhythmic transcripts were determined for the control and CLK8 treatment groups.

Common, vehicle or treatment specific cyclic treatments were annotated with KEGG with ClusterProfiler [77] package in R.4.2 with following parameters: MinGSSize =10, MaxGSSize=220, pvalueCutoff = 0.05 and qvalueCutoff = 0.2.

3.12. Statistical Analysis

Amplitude and period analysis of bioluminescence data determined with Biodare2[76]. Two-Way Anova and Student’s t-test were performed via GraphPad Prism (GraphPad Software, California, USA). Graphs constructed with mean and Standard

Error of Mean (SEM). There are at least 3 biological replicas for each experimental setup (n=3, ***p-value<0.001, **p-value<0.01, *p-value<0.05).

CHAPTER 4

RESULTS

4.1. Cell Viability Assessment

A previous study from my group showed CLK8 increased amplitude by reducing the interaction between CLOCK and BMAL1 [24]. Additionally, this study suggested that CLK8 might be used in aged organisms, where their circadian rhythm is highly reduced. To show the effect of CLK8 on circadian rhythm on aged cells I decided to use MRC5 (human lung fibroblast cells), used as a model cell line for the replicative senescence. Initially, I determined the nontoxic concentration of the CLK8 for MRC5 cell line using MTT assay. MRC5 cells were treated with different concentration CLK8, and then mitochondrial activity was measured. As shown in **Figure 4.1**, CLK8 was found to be nontoxic for the cells with concentration below 20 µM. Therefore 10 µM of CLK8 is selected throughout the studies.

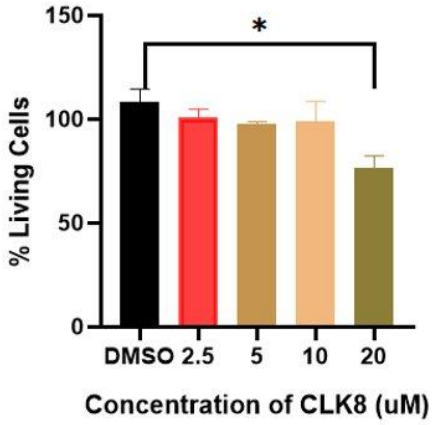

Figure 4.1. Determination of toxicity of CLK8 on MRC-5 cells. Cells with %70 confluency were treated with various dosages of CLK8 (0.25%DMSO). Following 48 hours of incubation, viability was measured by Synergy H1 Microplate Reader (Bio-Tek Instruments). All measurements were normalized to %0.25 DMSO control (Data represent the mean ± SEM; n=3).

4.2. The effect of CLK8 on cellular distribution of BMAL1 and CLOCK

The major effect of the CLK8 on CLOCK/BMAL1 is their cellular distribution by reducing the interaction between CLOCK and BMAL1 and, in turn, reduces the level of the CLOCK in the nucleus [24]. To confirm such an effect on MRC5 cells, cells treated with 10 µM of CLK8. After harvesting the cells, cellular fractions were performed to isolate cytosolic and nuclear proteins. Proteins, known to be specifically localized in nucleus (histone-H3) and cytoplasm (tubulin), were used as controls to evaluate the purity of the fractions (**Figure 4.2**). I then probed both fractions to anti-BMAL1 and anti-CLOCK to quantify their level in the presence of the CLK8. Consistent with our previous results, CLK8 causes the reduction of the CLOCK in the nucleus in the MRC-5 cell line (**Figure 4.2 B**).

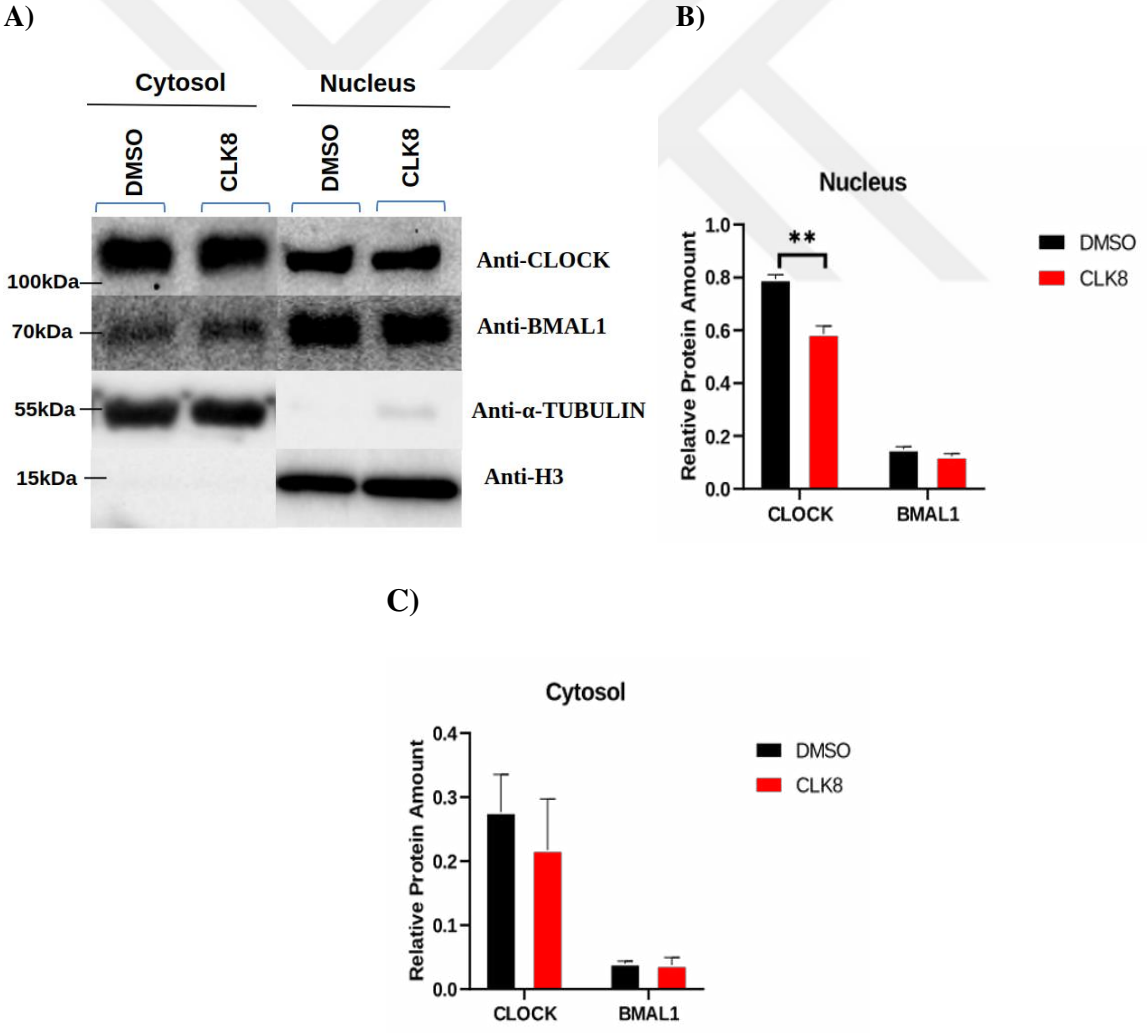

Figure 4.2. Effect of CLK8 on subcellular localization CLOCK and BMAL1. (A) Subcellular fractionation was performed on unsynchronized MRC-5 cells (PDL:61) with

10μM of CLK8 and 0.25% DMSO. Protein levels normalized according to levels of HISTONE H3 or α-TUBULIN. (B) Quantification of CLOCK and BMAL1 in cytoplasm and nucleus after CLK8 treatment. (Data are mean ± SEM; n=3, independent experiments. *p-value <0.05, versus the DMSO control by Student-t test)

These results suggested that CLK8 affects cellular distributions and had the same effect as previously described [24]. Therefore, I decided to test the effect of CLK8 on senescence.

4.3. CLK8 affect amplitude of the Circadian Rhythm in MRC5 during the senescence

MRC5 cell line is going into senescence around 64 population doublings [49,50]. To test the effect of CLK8 on senescence MRC5 cells were grown under two different conditions: The one in the presence of the CLK8 and the other one in the presence of the CLK8. The samples from each condition were taken to assess for circadian rhythm and senescence perspectives. Cells treated with CLK8 exhibited higher amplitude of circadian rhythm compared to DMSO treated cells at all population doubling time (PDL) without altered period length (**Figure 4.3 A, B, C, D**). To determine the level of the senescence at each PDL I performed β-gal assay. Results indicated that the number of the senescence cells were increased as PDL number increased. Notably, CLK8 treated cells had delayed senescence compared to DMSO treated cells (**Figure 4.3 E**).

A)

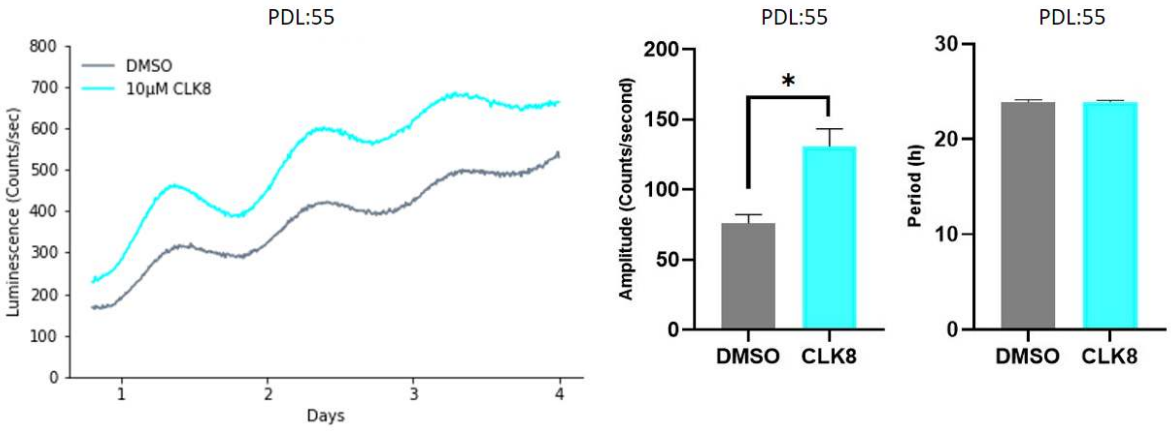

B)

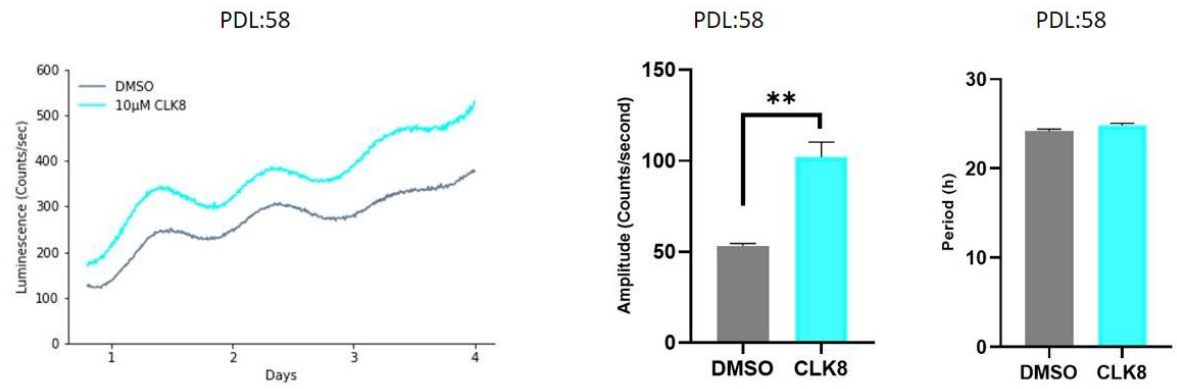
PDL:58
DMSO
10μM CLK8
Luminescence (Counts/sec)
Days
PDL:58
Amplitude (Counts/second)
**
DMSO
CLK8
PDL:58
Period (h)
DMSO
CLK8

C)

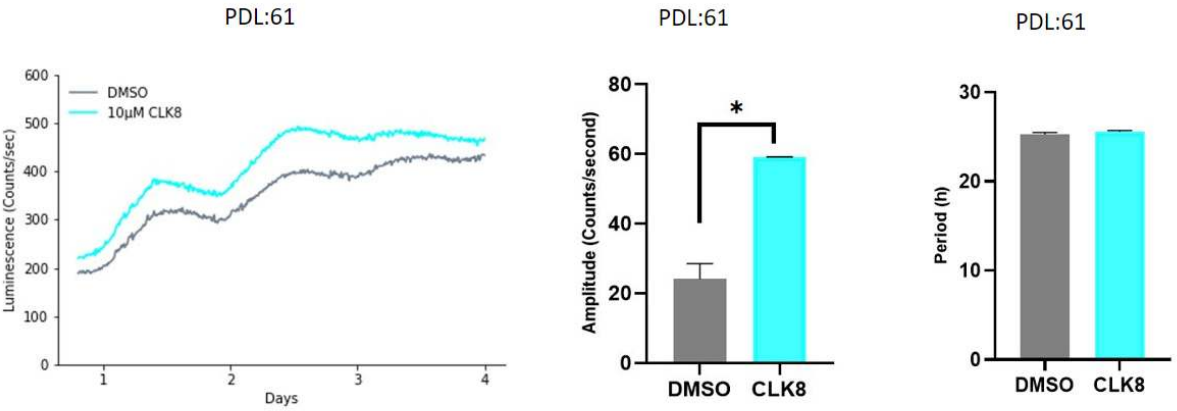
PDL:61
DMSO
10μM CLK8
Luminescence (Counts/sec)
Days
PDL:61
Amplitude (Counts/second)
*
DMSO
CLK8
PDL:61
Period (h)
DMSO
CLK8

D)

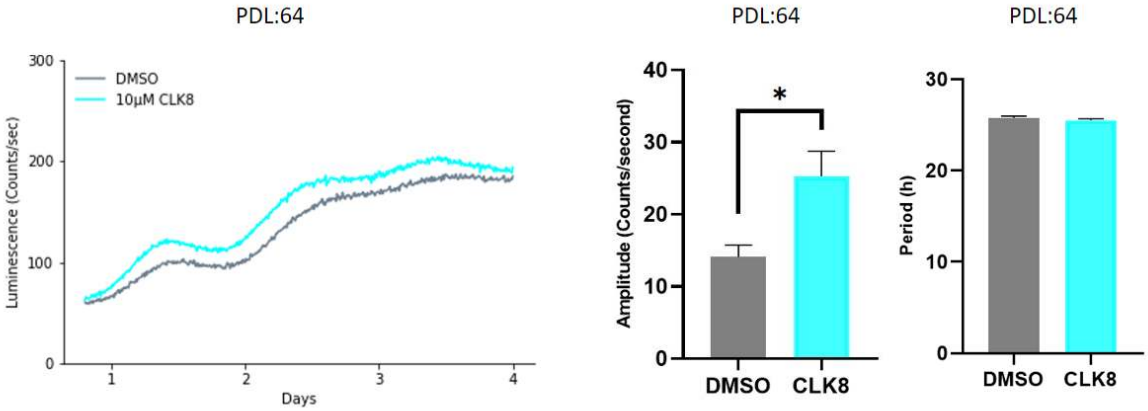
PDL:64
DMSO
10μM CLK8
Luminescence (Counts/sec)
Days
PDL:64
Amplitude (Counts/second)
*
DMSO
CLK8
PDL:64
Period (h)
DMSO
CLK8

E)

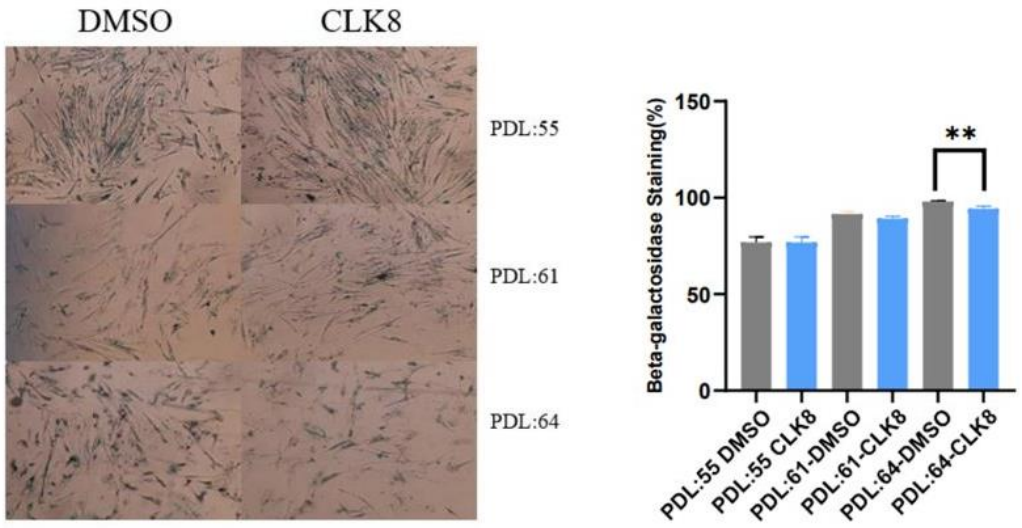

Figure 4.3 Effects of CLK8 on MRC-5 cells in different population doubling levels. (A, B, C, D) Continuous monitoring of circadian rhythms for five days in aging MRC-5 by Lumicycle (Actimetrics). *Bmal1*-d*Luc* is expressed by lentiviral infection. Cells were synchronized and treated with 10μM CLK8 and 0.25% DMSO. The data of the last day was omitted. Amplitude and periods were calculated via the Biodare2 repository [76]. Data represent the mean ± SEM; n=3. *p-value <0.05; **p-value <0.01.E) Representative images of beta-galactosidase staining. Stained and unstained cells were counted. Percentages of stained cells were quantified. Data represent the mean ± SEM; n=4. *p-value <0.05; versus the DMSO control by Student-t test.

4.4. Enhancement of Telomerase Activity and Lengthening of Telomere Length

MRC-5 cells enter senescence is chromosomal instability that arises from telomere shortening [74]. After observing the delayed senescence and enhancement of amplitude with CLK8, I hypothesized that CLK8 might interfere with telomere shortening and cause delay of senescence. To test that I collected the CLK8 and DMSO treated cells at the PDL of 55, 58, 61, and 64. Then I isolated chromosomal DNA and measured their telomere length using Absolute Telomere Length Quantification kit (Sciencell,8918). As seen in **Figure 4.4 A**, telomere length was shortening as PDL number was increased. However, telomere length was maintained in CLK8 treated cells. These results prompted me to check the telomerase

activity in these cells to attribute such differences with its activity. I measured telomerase activity from those cells using TeloTAGGG Telomerase PCR ELISA^{PLUS} kit (Roche,12013789001). Results indicated that telomerase activities significantly were higher in CLK8 treated cells **(Figure 4.4 B)**.

A) **B)**

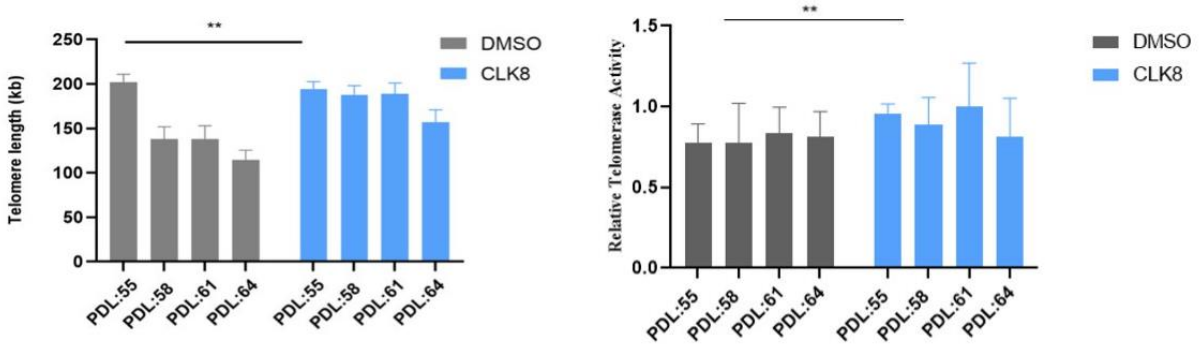

Figure 4.4. Telomere Length and Telomerase Activity are affected by CLK8 treatment. (A, B) Telomere lengths and relative telomerase activities of MRC5 cells were quantified for different population levels either treated with %0.25 DMSO or 10µM CLK8. Telomerase activities normalized to %0.25 DMSO. Data represent the mean ± SEM; n=3. *p-value <0.05; **p-value <0.01 versus the DMSO control by two-way ANOVA.

All these results suggested that CLK8 delay senescence maintaining the telomere length by increasing the telomerase activity. To gain more insight into the effect of CLK8 at genome-wide level, I decided to perform an RNA-seq experiment.

4.5. Time-dependent reprogramming of transcriptomics

To identify the pathways and genes affected solely by CLK8 in MRC5 cell line, circadian clock in the cells were reseted by dexamethasone and samples were collected at four different time points across 24 h. Then total RNA from CLK8 and DMSO-treated cells were isolated followed by poly A selection and library preparation. The quality of the library

was assessed by BioAnalyzer 2100 and then the samples were sequenced using Illumina Hiseq 2500 platform. After sequencing and de-multiplexing, RNA-seq data were aligned to the human reference genome (GRCh38) and gene expression values were calculated using STAR v2.5 with RSEM v1.3.0 [78]. An overview of the sequencing and mapping data for control and CLK8-treated is shown in **Table 4.1**. Because of low base call, I excluded CLK8_18_3 and DMSO_0_2 from further analysis.

Additionally, I performed Pearson correlation between all samples. Pearson correlation exhibited there are higher correlation between biological replicates (R^2 >0.8, **Figure 4.5**). I also investigated the percentage of genes that have expression in my data depending on chromosomal locations. Except from chromosome Y, data is distributed uniformly which suggest that expression data covers similar amount of genes all of the chromosomes (**Figure 4.6**).

Table 4.1. Summarizes the RNA-seq gene expression data across all samples.

Sample	Total Bases	Total Clean Reads	Uniquely Mapped Percentages	Q30 (%)
DMSO_0_1	17,341,848,680	29,237,877	94,10%	91,51%
DMSO_6_1	8,669,988,140	14,151,899	92,90%	92,16%
DMSO_12_1	15,814,075,980	18,552,617	94,30%	81,92%
DMSO_18_1	7,185,072,864	8,735,889	94,90%	81,51%
DMSO_24_1	10,139,654,228	23,530,628	95,70%	91,08%
CLK8_0_1	8,097,693,006	17,285,653	95,20%	92,43%
CLK8_6_1	8,674,186,544	12,891,317	95,20%	90,23%
CLK8_12_1	7,956,632,732	7,460,222	94,50%	81,65%
CLK8_18_1	147,376	170	95,30%	82,43%
CLK8_24_1	11,636,285,292	27,029,334	95,30%	91,87%
DMSO_0_3	9,718,507,074	22,683,019	96,10%	90,66%
DMSO_6_3	9,687,151,924	20,512,693	95,90%	91,37%

DMSO_12_3	8,711,406,232	19,947,211	95,80%	89,80%
DMSO_18_3	8,529,150,742	17,725,943	95,70%	91,12%
DMSO_24_3	7,790,378,108	16,811,461	95,20%	91,96%
DMSO_0_2	620,308	866	91,50%	87,53%
DMSO_6_2	6,931,285,050	11,029,116	92,90%	90,24%
DMSO_12_2	6,952,510,516	9,934,774	91,00%	89,15%
DMSO_18_2	6,546,463,362	8,739,924	94,40%	90,33%
DMSO_24_2	8,180,228,398	19,248,484	95,60%	90,25%
CLK8_0_2	7,634,835,122	14,223,254	88,20%	90,90%
CLK8_6_2	6,719,487,618	9,573,872	90,70%	90,04%
CLK8_12_2	6,812,167,492	10,055,041	91,60%	90,22%
CLK8_18_2	17,180,062,750	36,247,297	94,10%	90,37%
CLK8_24_2	10,803,491,300	24,638,804	95,60%	90,27%
CLK8_0_3	20,341,031,820	42,080,050	95,00%	88,76%
CLK8_6_3	9,080,016,862	18,711,091	95,30%	89,43%
CLK8_12_3	8,095,651,486	18,500,668	95,70%	89,89%
CLK8_18_3	10,046,139,626	21,578,993	94,50%	89,35%
CLK8_24_3	11,132,802,670	27,962,607	93,80%	89,51%

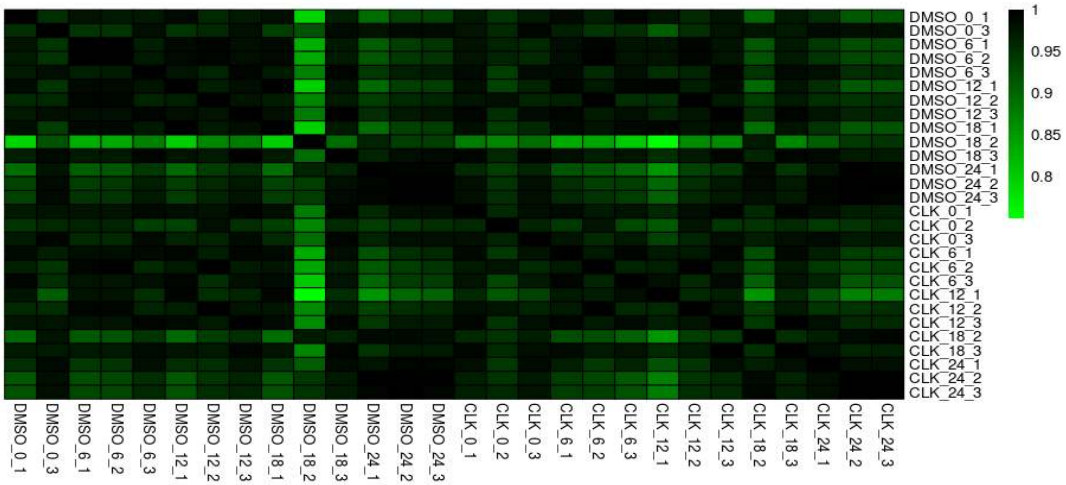

Figure 4.5 Heatmap of Pearson's correlation between samples. Biological replicates exhibit higher correlation in each other (R^2 >0.8).

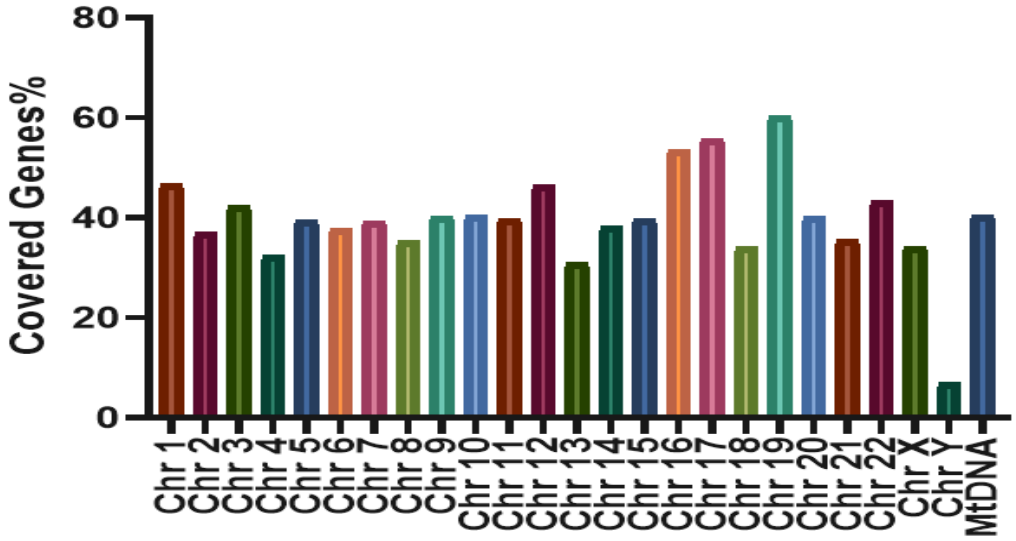

Figure 4.6 Percentages of genes in each chromosome covered in RNA-seq expression data.

All these analyses suggested that RNA-seq data from all samples had good quality and therefore I decided to proceed further analyses.

To identify rhythmically expressed genes, I used the MetaCycle package and meta2d function [79]. Cycling transcripts with significant p-values were detected and split according to their presence in either control or CLK8 treated group. Expression levels of core clock genes, *BMAL1, CRY2, PER2, NR1D* are rhythmically expressed in both conditions **(Figure 4.6, D).** These results validate cells are successfully reseted and genes are being oscillate in circadian rhythm manner. Our previous results indicate that expression of E-box controlled genes have damped compared to control [24]. Except *NR1D1,* these dampenings are clearly observable **(Figure 4.6, D)**. However, other core clock components or isoforms have not been detected as cycling.

Then I determined the number of genes that being expressed rhythmically. A total of 1518 genes were found to be rhythmic in DMSO treated cells while in CLK8 treated cells a

total 2739 genes are identified as rhythmically expressed genes accounting for 10.6% and 19.2% of the total number of expressed genes, respectively.

A)

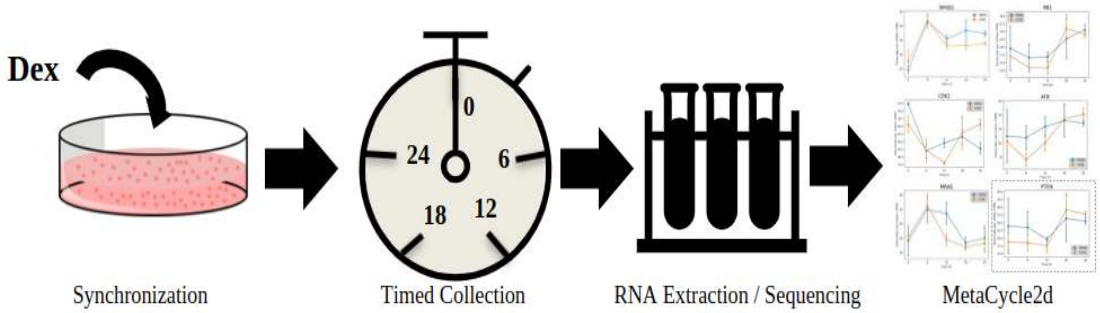

B)

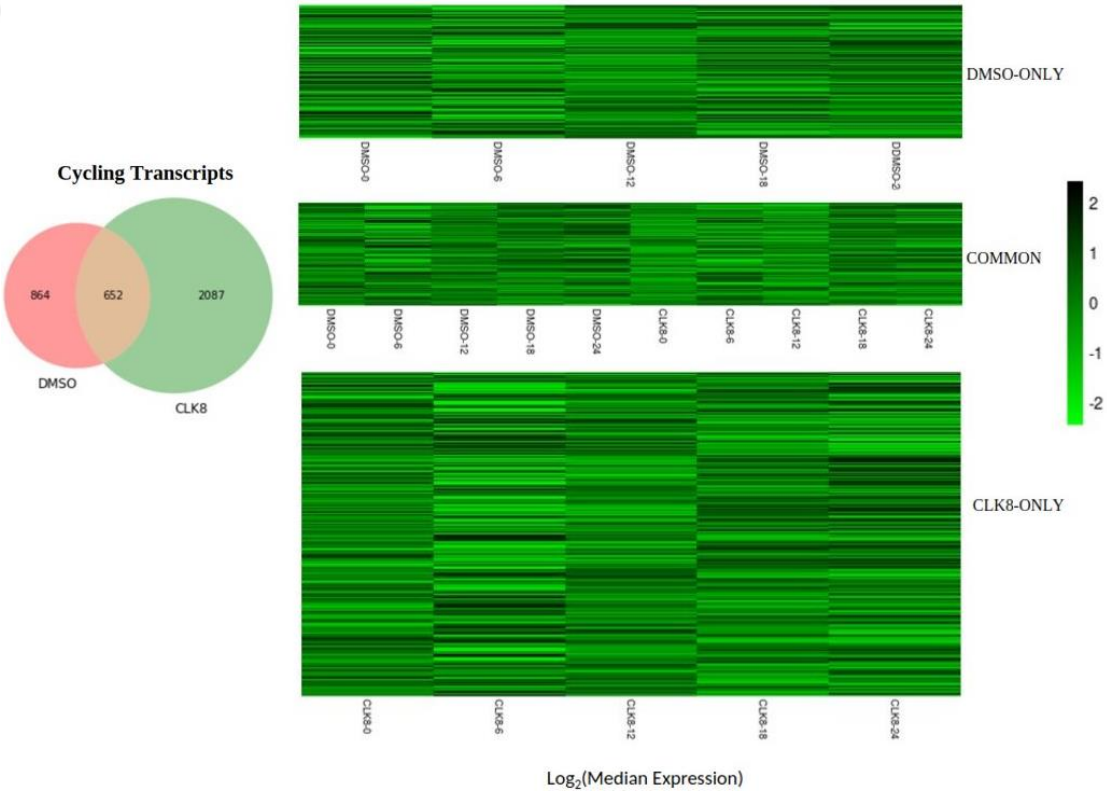

C)

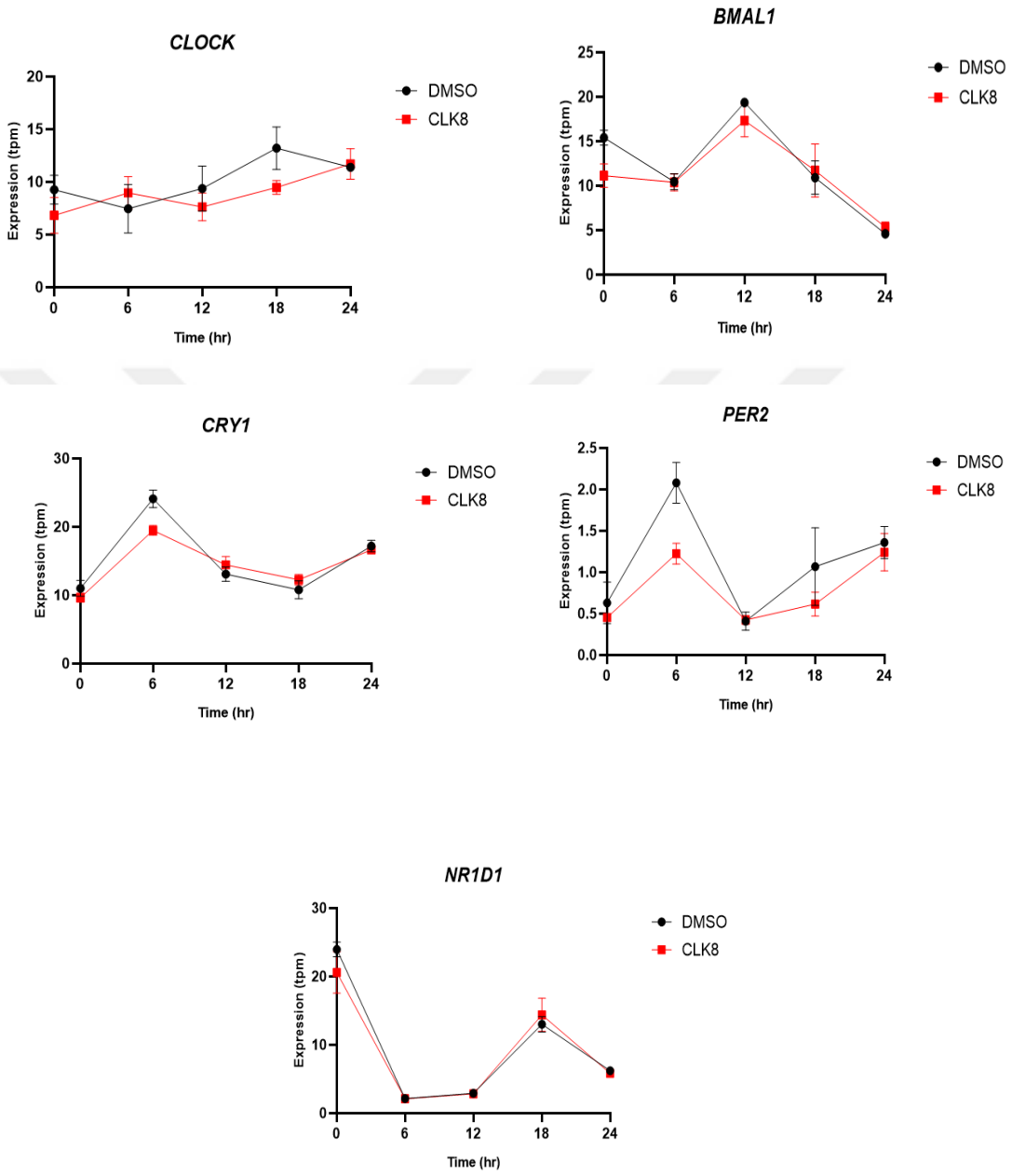

Figure 4.7. Schematic representation of sample collection and rhythmic transcripts. (A) Samples collected and sequenced for DMSO and CLK8 group at PDL:61. (B) Venn diagrams represent the number of cycling genes determined by Meta2d. Heat maps for cyclic genes constructed according to log2(MedianExpression) normalization via R pheatmap package [108]. (D) Except CLOCK, core clock genes are cyclic in both groups. Data collected from n>=2 biological replicates. All error bars represent SEM. p-value <0.05

versus DMSO control by two-way ANOVA analysis. TPM; Transcript per million, Dex; dexamethasone.

4.6. Determination of rhythmically expressed pathways by Kyoto Encyclopedia of Genes and Genomes (KEGG) Pathway-Gene Ontology (GO) analyses

To functionally categorize rhythmically expressed genes in cells treated with DMSO and CLK8, a GO term analysis was performed using the CusterProfiler package [77]. The assigned GO terms were used to classify functions of the rhythmically expressed genes based on KEGG pathways they involved.

KEGG Pathway Ontology analysis revealed numerous genes still persist in their rhythmic expression after CLK8 treatment. These top 10 pathways include protein processing in endoplasmic reticulum (hsa04141), biosynthesis of unsaturated fatty acids (hsa01040), viral carcinogenesis (hsa05203), cell cycle (hsa04110), cellular senescence (hsa04218), pancreatic cancer (hsa05212), nucleocytoplasmic transport (hsa03013), ribosome (hsa03008), mRNA surveillance (hsa03015) and colorectal cancer (hsa05210) pathways **(Figure 4.7 A)**.

After that, we primarily focused on the cellular senescence pathway since we had already demonstrated the effect of CLK8 on both cellular senescence and replicative senescence **(Fig.4.3E, Fig 4.4 A, B).** Through these genes, we examined how their rhythmicity is affected through aging [82]. 10 out of 32 cellular senescence genes show rhythmic expression patterns in young mice and lose their rhythmicity in aged mice at least in two different tissues [83]. Their rhythmicity is conserved via CLK8 treatment (**Table A1**). We further confirmed that 9 of these genes are rhythmically expressed in CLK8 treated cells but not in control via qPCR.

A)

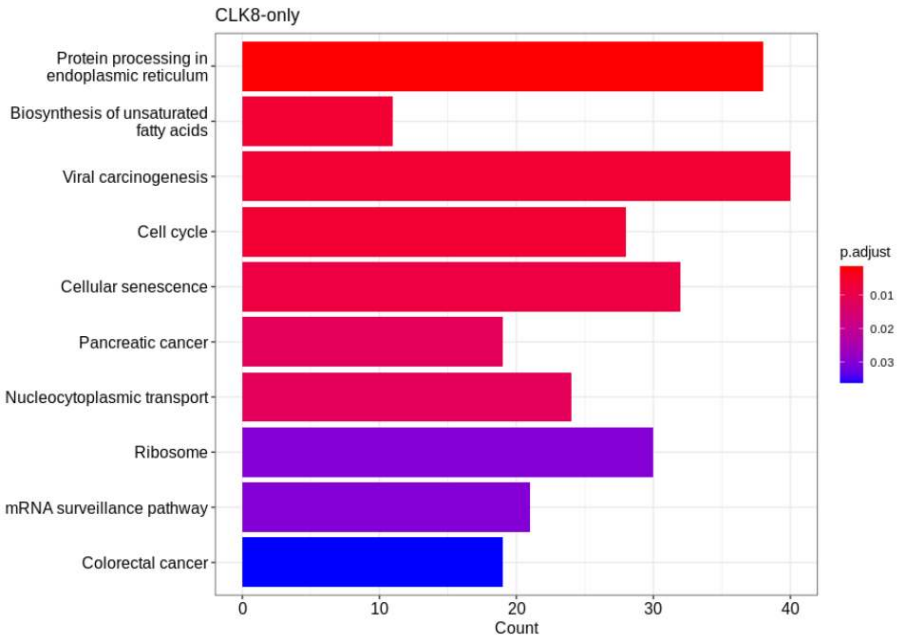
CLK8-only
Protein processing in endoplasmic reticulum
Biosynthesis of unsaturated fatty acids
Viral carcinogenesis
Cell cycle
Cellular senescence
Pancreatic cancer
Nucleocytoplasmic transport
Ribosome
mRNA surveillance pathway
Colorectal cancer
0
10
20
30
40
Count
p.adjust
0.01
0.02
0.03

B)

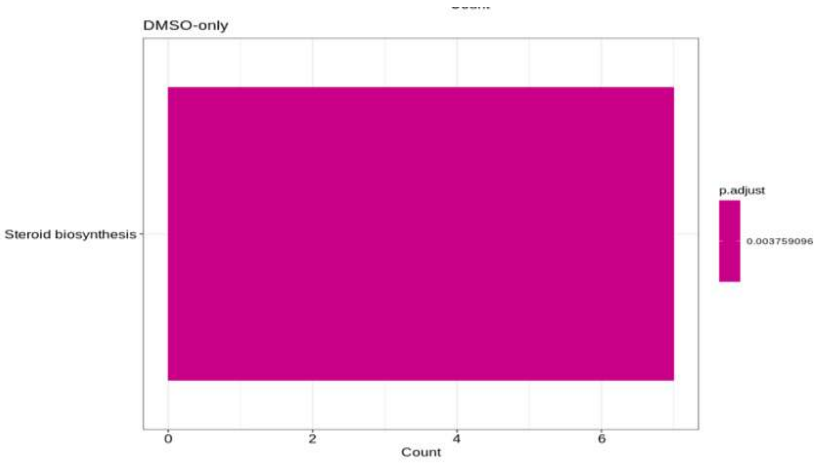
DMSO-only
Steroid biosynthesis
0
2
4
6
Count
p.adjust
0.003759096

C)

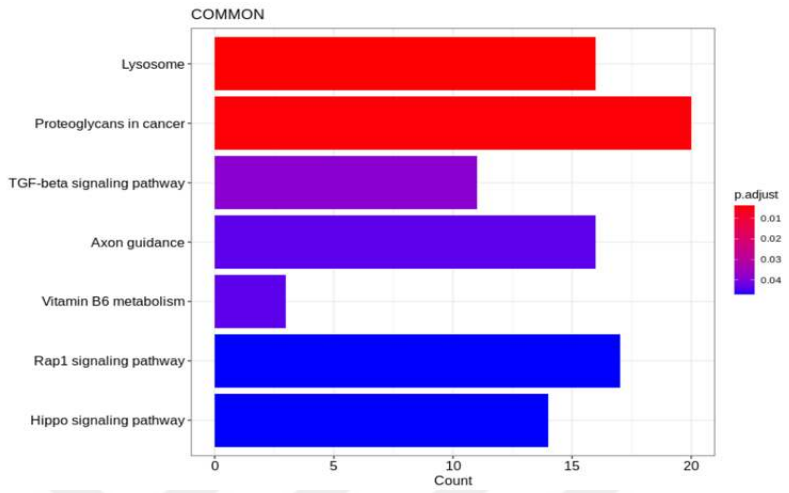

Figure 4.8. KEGG Ontologies of Cycling Transcripts. (A, B, C) The number of cycling genes is analyzed in KEGG Pathways and split as group-specific and common. Data represented with 0.05 and 0.02 p-value, q value cutoff.

Senescence Associated Genes	Age Declined Genes	qPCR Validated Age Declined Genes
CDK2	CDK2	CDK2
MRAS	MRAS	MRAS
ATR	ATR	ATR
NFKB1	NFKB1	NFKB1
PTEN	PTEN	PTEN
NRAS	NRAS	NRAS
TGFBR2	TGFBR2	TGFBR2
HIPK1	HIPK1	HIPK1
RB1	RB1	RB1
TRPM7	TRPM7	
MYC		
CDKN1A		
CDKN1B		
FOXO3		
CCNE2		
HLA-C		
MRE11		
PIK3CB		
TGFB2		
CDK6		
PPP3CB		
AKT3		
CCND2		
KRAS		
PPP3CA		
SLC25A6		
PPP1CA		
SMAD2		
PPP1CC		
PPP1CB		
LIN37		
RBBP4		

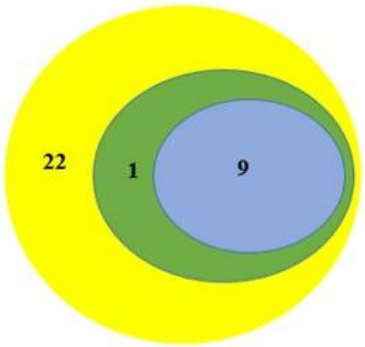

Figure 4.9. Rhythmically expressed genes in CLK8 treatment are associated with cellular senescence pathway. List of genes associated with cellular senescence pathway in KEGG database (hsa04218) [81]. The ones that lose rhythmicity with time are indicated as age-declined [82] and rescued with the treatment of CLK8 indicated at qPCR-validated aged decline genes. Venn Diagram represents the amount of senescence-associated cycling genes in CLK8 treatment, yellow; all senescence associated genes, green; age-declined genes, red; q-PCR validated genes.

4.7. Expression Profiles and q-PCR Validations of Selected Senescence Associated Genes

RNA-seq analyses and further qPCR validation reveal that cyclic expression has been comparatively more conserved in CLK8 treated cells. PDL:57 age is selected as a young group to compare alterations of rhythmic expression through treatments and aging.

A) **B)**

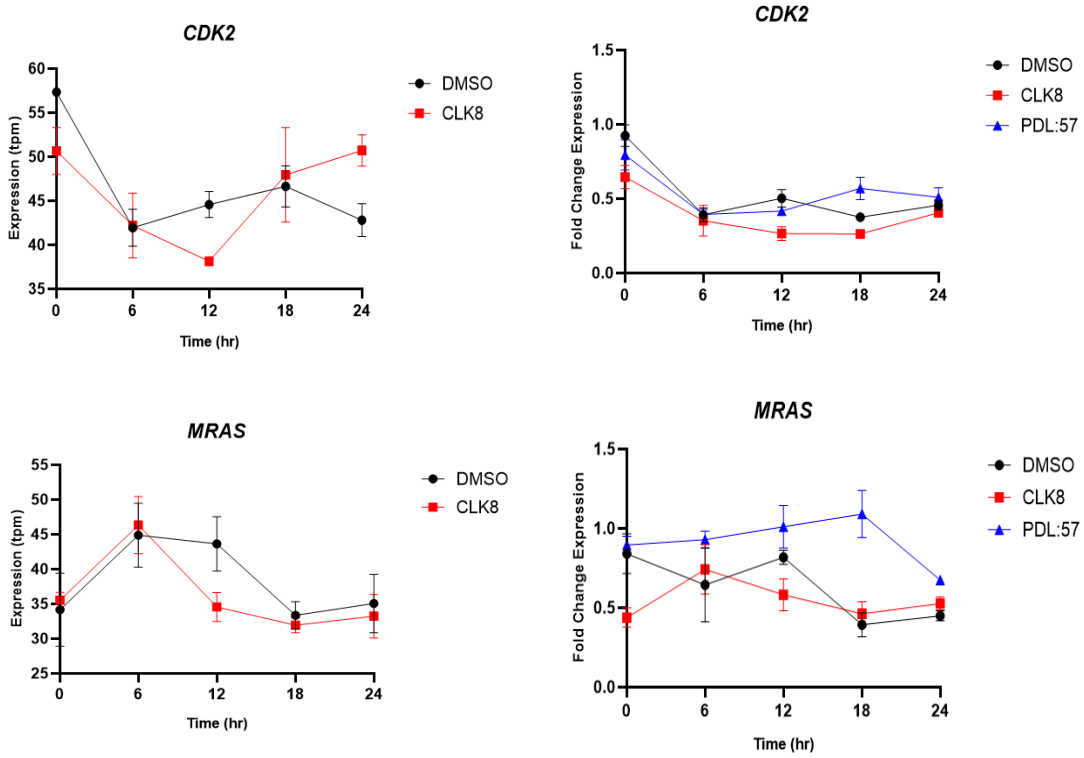

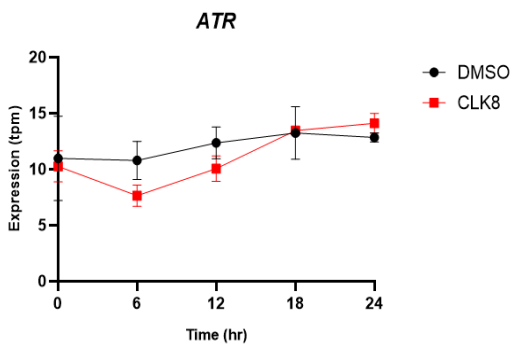
ATR
Expression (tpm)
Time (hr)
DMSO
CLK8

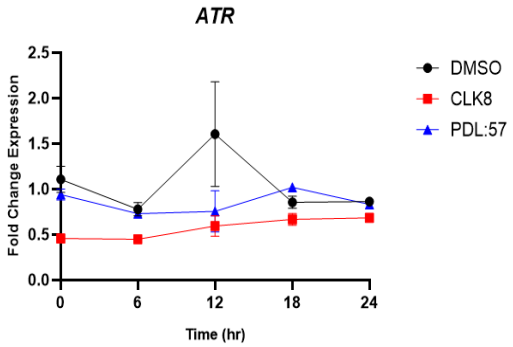
ATR
Fold Change Expression
Time (hr)
DMSO
CLK8
PDL:57

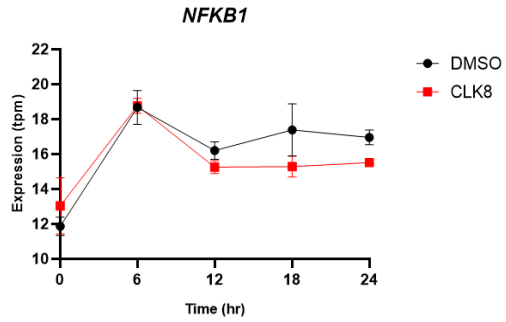
NFKB1
Expression (tpm)
Time (hr)
DMSO
CLK8

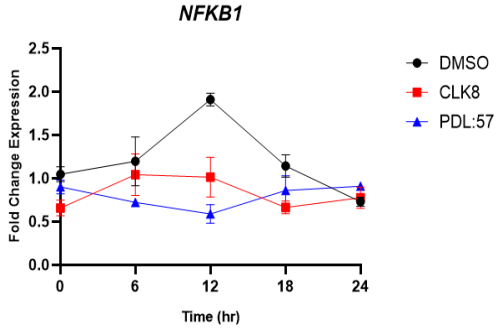
NFKB1
Fold Change Expression
Time (hr)
DMSO
CLK8
PDL:57

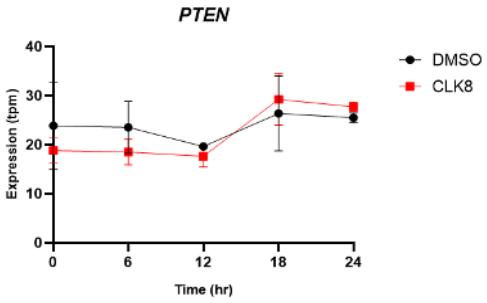
PTEN
Expression (tpm)
Time (hr)
DMSO
CLK8

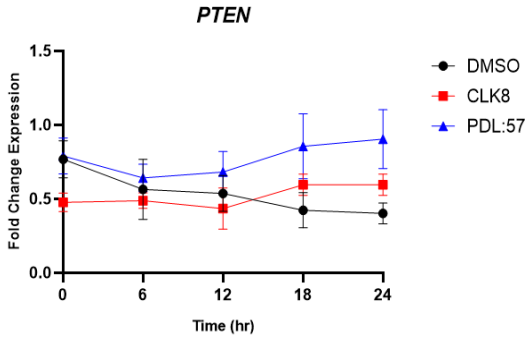
PTEN
Fold Change Expression
Time (hr)
DMSO
CLK8
PDL:57

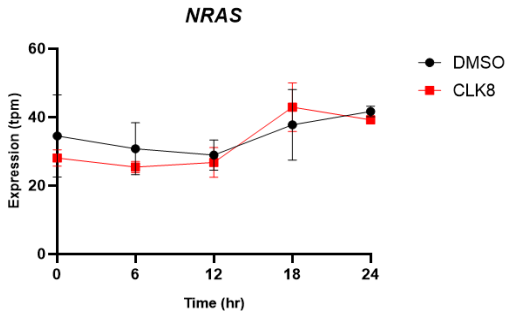
NRAS
Expression (tpm)
Time (hr)
DMSO
CLK8

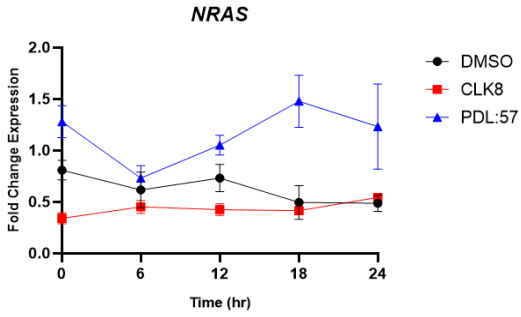
NRAS
Fold Change Expression
Time (hr)
DMSO
CLK8
PDL:57

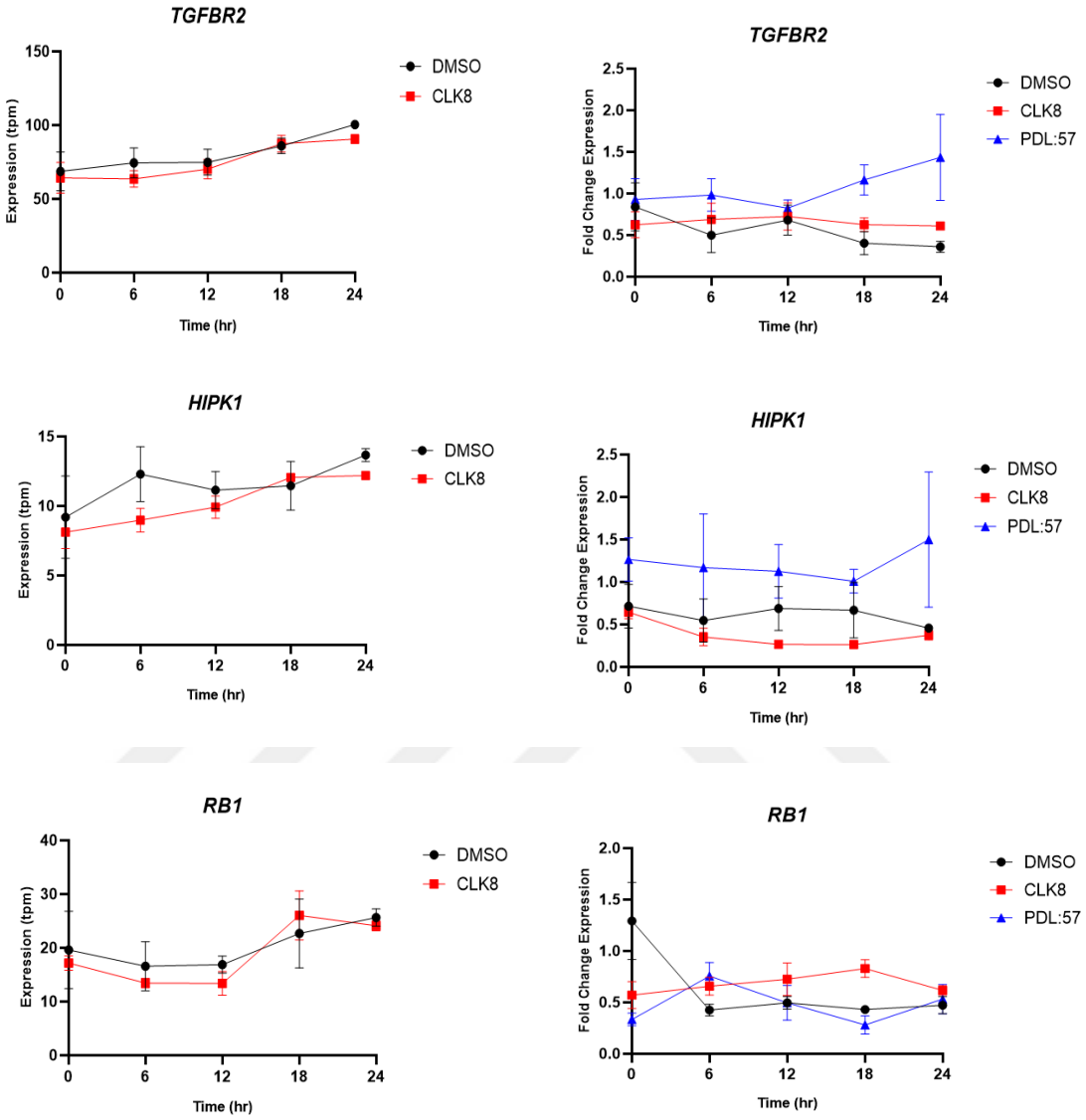

C)

PDL:57							
Label	**Rhythmic**	**BH p**	**Tau**	**P.Shape**	**P.Period**	**P.Peak**	**P.Trough**
Cdk2	TRUE	0.03535	0.74	COS	24	18	6
Mras	TRUE	0.03535	0.74	COS	24	14	2
Atr	TRUE	0.03356	0.95	COS	24	18	6
Nfkb1	TRUE	0.03535	0.8	COS	24	22	10
Pten	TRUE	0.03535	0.8	COS	24	22	10
Nras	TRUE	0.03356	0.95	COS	24	18	6
Tgfbr2	TRUE	0.03356	0.95	COS	24	2	14
Hipk1	TRUE	0.03535	0.74	COS	24	2	14
Rb1	TRUE	0.03535	0.74	COS	24	18	6

DMSO							
Label	**Rhythmic**	**BH p**	**Tau**	**P.Shape**	**P.Period**	**P.Peak**	**P.Trough**
Cdk2	FALSE	0.27266	0.4	COS	24	22	10
Mras	FALSE	0.3121	0.32	COS	24	6	18
Atr	FALSE	0.3121	0.2	COS	24	16	4
Nfkb1	FALSE	0.05034	0.95	COS	24	12	0
Pten	FALSE	0.27266	0.4	COS	24	22	10
Nras	FALSE	0.3121	0.2	COS	24	16	4
Tgfbr2	FALSE	0.3121	0.2	COS	24	16	4
Hipk1	FALSE	0.17706	0.6	COS	24	16	4
Rb1	FALSE	0.17706	0.6	COS	24	22	10

CLK8							
Label	**Rhythmic**	**BH p**	**Tau**	**P.Shape**	**P.Period**	**P.Peak**	**P.Trough**
Cdk2	TRUE	0.03928	0.8	COS	24	22	10
Mras	TRUE	0.03928	0.74	COS	24	6	18
Atr	TRUE	0.03928	0.8	COS	24	16	4
Nfkb1	TRUE	0.03928	0.74	COS	24	6	18
Pten	TRUE	0.03928	0.95	COS	24	2	14
Nras	TRUE	0.03928	0.74	COS	24	6	18
Tgfbr2	TRUE	0.03928	0.8	COS	24	10	22
Hipk1	TRUE	0.03928	0.74	COS	24	6	18
Rb1	TRUE	0.03928	0.74	COS	24	14	2

Figure 4.10. Expression Profiles of Targeted-Senescence Associated Genes. (A, B) RNA-seq and q-PCR expression levels of cellular senescence-related genes that has rhythmicity after CLK8 treatment and in PDL:57. DMSO treated groups show no rhythmicity. (C) JTK Cycle analysis results for selected genes among PDL:57, control and CLK8 treated groups. Data represent the mean ± SEM; n ≥ 2. *BH p-value <0.05. Treated groups data were normalized to DMSO and PDL:57 was normalized independently. Rhythmicity of q-PCR results has been confirmed by JTK Cycle with cosx 4h function by BioDare2 repository [76].

To decrease the false discovery rate of p-values, I used Benjamini-.Hochberg procedure and ranked p-values indicate there is no rhythmic expression pattern in DMSO-treated cells with respect to cosx 4h function (**Figure 4.9, C**). The 90% of targeted cells show cyclic pattern in just PDL:57 and CLK8-treated groups which importantly reveals the conservation of these senescence associated genes rhythmicity's with CLK8 treatment. Circadian clock as a vast controlling system starts to show abnormalities in aging but I showed that this phenotype is rescued by CLK8-treatment. Therefore, circadian control of

transcription is also enhanced in these cells which further supports the decrease in senescence cells in CLK8-treatment.

CHAPTER 5

DISCUSSION

Drug developments against aging have been challenging because of the complexity of the process. Almost all the biological pathways are directly affected by aging. The circadian clock is the central biological controlling system, and its power declines through aging. Restoring the power of the circadian clock has never been tried before because of the lack of appropriate drugs/systems. Even though numerous small molecules change the circadian phenotype, CLK8 is the only identified molecule that solely affects amplitude [24,41]. Amplitude damping is a significant abnormality in circadian rhythms that is observed with advanced age [61,64]. This dampening disrupts all the control mechanisms progressively. Reasons for controlled decay of circadian rhythms still cannot be understood [86,87]. CLK8 provides robust and enhanced circadian rhythm by affecting the stoichiometry of CLOCK:BMAL1 heterodmier in the nucleus [24]. This suggests that the abnormalities of circadian rhythms through aging would be directly related with distribution of core clock proteins in the nucleus.

Dampening and period lengthening are two important abnormalities of the circadian clock through aging [60,61]. I also observed this age-dependent decline in MRC-5 cells which is rescued by CLK8 treatment (**Figure 4.3**). Core clock components deficiencies directly reduce the lifespan of mice [88]. Moreover, both expression and protein levels of CLOCK and BMAL1 substantially change during aging which lead to abolishment of rhythms in tissue dependent manner [88]. Rhythmically expressed genes are down regulated with aging in mice [82]. I delayed this downregulation by changing the stoichiometry of CLOCK:BMAL1 in the nucleus through CLK8 treatment in MRC-5 cells (**Figure 4.6 B**).

Compared to the control group, almost a 2-fold increase was observed in rhythmic genes that play crucial roles in various pathways (**Figure 4.7**). Throughout these pathways, proteins that take place in cell cycle and cellular senescence directly correlate with aging and cellular arrest. When I compared the expression of these 10 genes that are involved in cellular

senescence pathway (hsa04218) in relatively young MRC-5 cells (PDL:57), I detected that their expression is cycling, but they lose their rhythmicity in aging. However, CLK8 treatment rescued 9 of them. Among them, CDK2, NFKB1 and PTEN can be representative examples of the importance of these genes. For instance, CDK2 is a cycling gene that starts to lose its cyclicity with age in mice [82]. CDK2 is one of the key players in cellular senescence control and alterations in CDK2 integrity/levels would be directly associated with either senescence or tumorigenesis [89,90,91]. Therefore, conservation of CDK2 rhythmicity could contribute to delayed senescence and progression of cell cycle with CLK8 treatment (**Figure 4.9 B**).

NFKB1 is also another important factor involved in the regulation of both inflammation and aging/cellular senescence. NFKB1$^{-/-}$ mouse exhibit increased SASPs and telomere damage [92,93]. Loss of p50/Nfkb1 leads to decrease in cellular apoptosis and increases senescence associated with premature aging in mice [94]. Therefore, control of the cyclic expression status of NFKB1 would be important in terms of increasement of cellular apoptosis and decrease in SASPs phenotype which are provided through CLK8 treatment [82] (**Figure 4.9 B**).

PTEN is a phosphatase that acts as a tumor suppressor, and it is involved in the decrease of oxidative stress [95]. Furthermore, PTEN decreases the glycosylation which is enhanced in both cancer and senescence cells [96]. Even though the expression of PTEN is rhythmic in both humans and mice, its abolishment would be related with intolerability of oxidative stress in aging [82,97]. Therefore, conservation of PTEN cyclicity would further decrease the chromosomal instability through oxidative stress in CLK8 treatment. Additionally, PTEN rhythmicity would decrease the enhanced glycosylation preference in CLK8 treated cells.
The relation between cellular senescence associated genes and circadian clock through the aging process is still not fully understood [104-107]. Even though they directly interact or exist in rhythmic expression patterns, expression differentiations through aging might be affected by epigenetic regulations [101,102]. Moreover, epigenetic clocks and their effects on core clock gene expressions needs to be further investigated [103].

Integrity of telomere sequences depends on various factors that are associated with telomere sequences or regulating telomere-binding proteins [55-57]. Several components of shelterin complex show rhythmic expression. However, they show tissue dependencies and their dampening with aging is not clearly understood [82]. TERF1 and TERF2 are two telomere binding proteins that decrease the accumulation of DNA damage and increase the stability at telomere sequences [56] (**Figure 2.3**). Expression of TERF1 shows cyclicity in CLK8 treatment [**Figure C1**] that would play an important role in the conservation of telomere integrity. Circadian rhythms control both telomeres and telomerase activity in HEK293T cells [98]. However, the activity of telomerase in somatic cells is restricted or at low levels [99,100]. Therefore, it might be the reason why I did not detect any cycling subunits of telomerase holoenzyme either in control or CLK8 treatment via RNA-seq. Their expressions would be further investigated with q-PCR for better resolution.

Even though CLK8 treatment reprograms rhythmic expression in MRC-5 cells, I focused on cellular senescence related genes in this thesis. Through these genes, I only focused on those whose rhythmicity was lost through aging that was determined in mice [82]. However, there would be differences in aged dependent regulations of these genes in human and mice. Therefore, age dependent rhythmicity of other senescence associated genes needs to be further analyzed in human. On the other hand, there are various pathways that persist rhythmicity in CLK8 treatment. Their roles in aging could be further illuminated.

Genes that still persist rhythmic expression in CLK8 treatment directly or indirectly regulate the causes of senescence such as oxidative stress, DNA damage and cell cycle arrest [89-97]. Conservation of these rhythmic genes under the circadian clock further delay the senescence phenotype. Therefore, CLK8 stands as a precious candidate for future anti-aging drug developments.

APPENDICES

APPENDIX A: Age-Declined Genes

Table A.1 Genes demonstrate loss of rhythmicity in aging in cellular senescence pathway [82].

Gene	Tissue	Group	Amplitude	Phase	Peak Time	Basal	p-value
CDK2	kidney	young	0.153	22.8	7.15	4.13	0.0500
CDK2	kidney	aged	0.170	23.0	7.01	4.23	0.0201
CDK2	kidney	old	0.134	21.2	8.80	4.31	0.353
CDK2	hypothalamus	young	0.235	1.18	4.82	2.39	0.00981
CDK2	hypothalamus	aged	0.143	22.1	7.86	2.38	0.175
CDK2	hypothalamus	old	0.138	17.7	12.3	2.36	0.328
MRAS	hypothalamus	young	0.104	7.00	23.0	7.07	0.0256
MRAS	hypothalamus	aged	0.0804	7.58	22.4	7.02	0.0953
MRAS	hypothalamus	old	0.0585	6.96	23.0	6.99	0.534
MRAS	heart	young	0.153	4.34	1.66	3.21	0.0510

MRAS	heart	aged	0.167	8.08	21.9	3.30	0.00759
MRAS	heart	old	0.124	3.20	2.80	3.29	0.308
ATR	kidney	young	0.0949	23.3	6.75	5.19	0.150
ATR	kidney	aged	0.234	20.7	9.29	5.14	0.000253
ATR	kidney	old	0.176	22.4	7.55	5.02	0.0628
ATR	muscle	young	0.144	16.5	13.5	3.40	0.0000457
ATR	muscle	aged	0.174	22.5	7.54	3.36	0.151
ATR	muscle	old	0.305	2.65	3.35	3.61	0.0962
NFKB1	hypothalamus	young	0.179	21.4	8.60	4.88	0.0753
NFKB1	hypothalamus	aged	0.177	20.1	9.91	4.90	0.156
NFKB1	hypothalamus	old	0.0492	21.3	8.67	4.87	0.891
NFKB1	heart	young	0.0775	3.43	2.57	5.74	0.0554
NFKB1	heart	aged	0.0551	6.86	23.1	5.83	0.383
NFKB1	heart	old	0.129	2.27	3.73	5.95	0.188
PTEN	kidney	young	0.0846	13.9	16.1	7.40	0.00664
PTEN	kidney	aged	0.0640	17.5	12.5	7.47	0.177
PTEN	kidney	old	0.0393	17.9	12.1	6.40	0.940

PTEN	lung	young	0.163	18.3	11.7	7.48	0.0204
PTEN	lung	aged	0.138	18.2	11.8	7.46	0.0378
PTEN	lung	old	0.355	20.0	10.0	6.72	0.279
NRAS	kidney	young	0.132	23.2	6.79	5.57	0.0575
NRAS	kidney	aged	0.0895	0.580	5.42	5.64	0.339
NRAS	kidney	old	0.0787	24.0	6.04	5.39	0.570
NRAS	lung	young	0.102	21.4	8.61	7.10	0.0485
NRAS	lung	aged	0.0778	21.0	8.99	7.09	0.0723
NRAS	lung	old	0.162	20.7	9.28	6.74	0.284
TGFBR2	hypothalamus	young	0.183	3.07	2.93	4.46	0.0284
TGFBR2	hypothalamus	aged	0.169	8.28	21.7	4.66	0.0620
TGFBR2	hypothalamus	old	0.0782	21.3	8.73	4.76	0.889
TGFBR2	kidney	young	0.124	0.324	5.68	7.02	0.0797
TGFBR2	kidney	aged	0.152	23.5	6.54	7.03	0.198
TGFBR2	kidney	old	0.0645	23.0	7.01	6.97	0.691
HIPK1	kidney	young	0.126	11.3	18.7	7.55	0.0330

HIPK1	kidney	aged	0.149	16.9	13.1	7.55	0.132
HIPK1	kidney	old	0.129	16.9	13.1	7.07	0.227
HIPK1	muscle	young	0.178	15.7	14.3	6.24	0.00278
HIPK1	muscle	aged	0.234	14.8	15.2	6.10	0.0628
HIPK1	muscle	old	0.229	2.94	3.06	5.75	0.297
RB1	kidney	young	0.0925	3.45	2.55	5.60	0.0552
RB1	kidney	aged	0.0937	0.394	5.61	5.70	0.235
RB1	kidney	old	0.165	2.72	3.28	5.38	0.512
RB1	hypothalamus	young	0.135	2.53	3.47	5.21	0.0359
RB1	hypothalamus	aged	0.213	6.79	23.2	5.16	0.000761
RB1	hypothalamus	old	0.250	22.9	7.05	4.77	0.433
TRPM7	hypothalamus	young	0.142	21.6	8.44	5.97	0.0231
TRPM7	hypothalamus	aged	0.0449	20.9	9.08	5.91	0.835
TRPM7	hypothalamus	old	0.320	21.7	8.27	5.25	0.366
TRPM7	muscle	young	0.368	17.0	13.0	6.03	0.000968
TRPM7	muscle	aged	0.313	18.9	11.1	6.06	0.0118
TRPM7	muscle	old	0.263	0.910	5.09	5.84	0.403

APPENDIX B: Primer Sequence

Table B 1. Primer sequences.

Gene	Real-Time Primer Sequences
CDK2	F: 5'-GGACGGAGCTTGTTATCGCAAA-3' R: 5'-CACTGGAGGAGAGGGTGAGAT-3'
MRAS	F: 5'-CTTGGACGTTCTGGACACAGCT-3' R: 5'-CTGTCTTTGACGCGCAGG-3'
ATR	F: 5'-GCTTGGGACTGCTTTGTTCG-3' R: 5'-TGCACAGCATCCCTGTTTTC-3'
NFKB1	F: 5'-ATGTGGGACCAGCAAAGGTT-3' R: 5'-GTTTGCGAAGCCGACCAC-3'
PTEN	F: 5'-AGGATGGATTCGACTTAGACTTGA-3' R: 5'-AAAGGATATTGTGCAACTCTGC-3'
NRAS	F: 5'-TGGTGATGTAACAAGATACT-3' R: 5'-ACTAAACTACTGAGAGCTGG-3'
TGFBR2	F: 5'-GCACGTTCAGAAGTCGGATG-3' R: 5'-CTGCACCGTTGTTGTCAGTG-3'
HIPK1	F: 5'-TATGTCCACCTGCGTTTCAA-3' R: 5'-GTACAGCTTCCCTGCGTGA-3'
RB1	F: 5'-GCATGGCTCTCAGATTCACCT-3' R: 5'-GCAGTGTGATTATTCTGGAGAGGA-3'
TRPM7	F: 5'-GCCCTACCGACCAAAGATTGA-3' R: 5'-CCTCTTCATAAGGCAAGCCCA-3'

APPENDIX C: TERF1 and DKC1 Expression

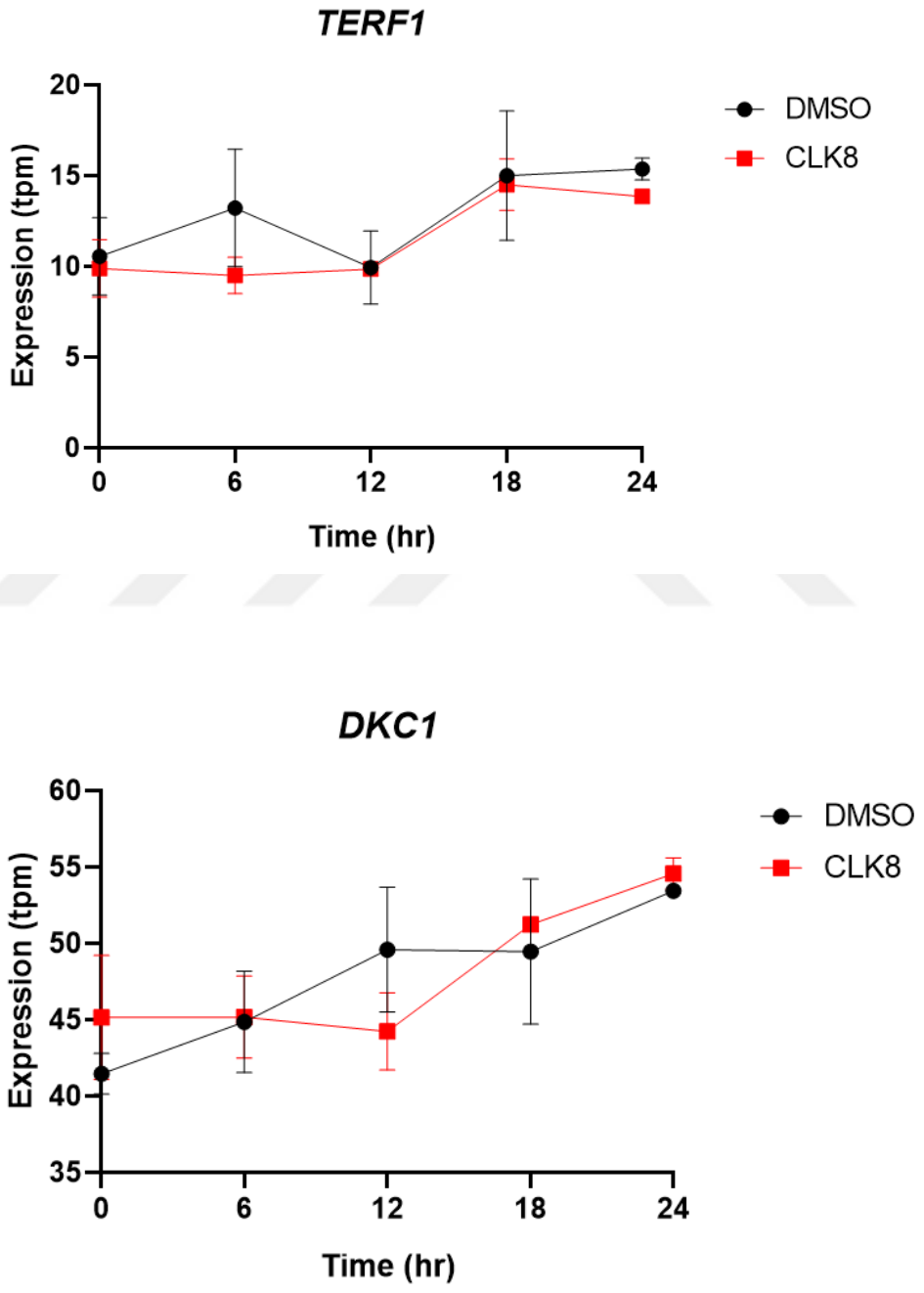

Figure C 1.RNA-seq expression levels of telomere, telomerase related genes. Data show rhythmicity only in CLK8 treatment.

APPENDIX D: Protein markers

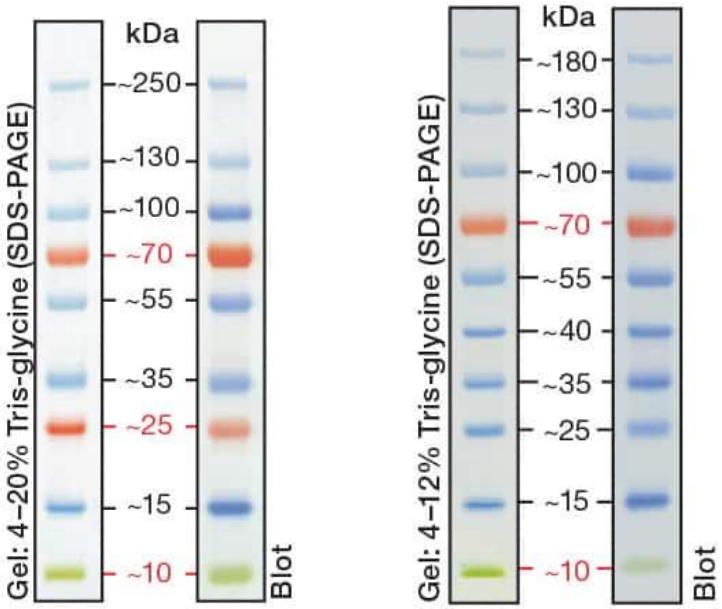

Figure D 1. Protein markers that were used throughout the study (from Thermo Sciencific).

APPENDIX E: Expression Vectors

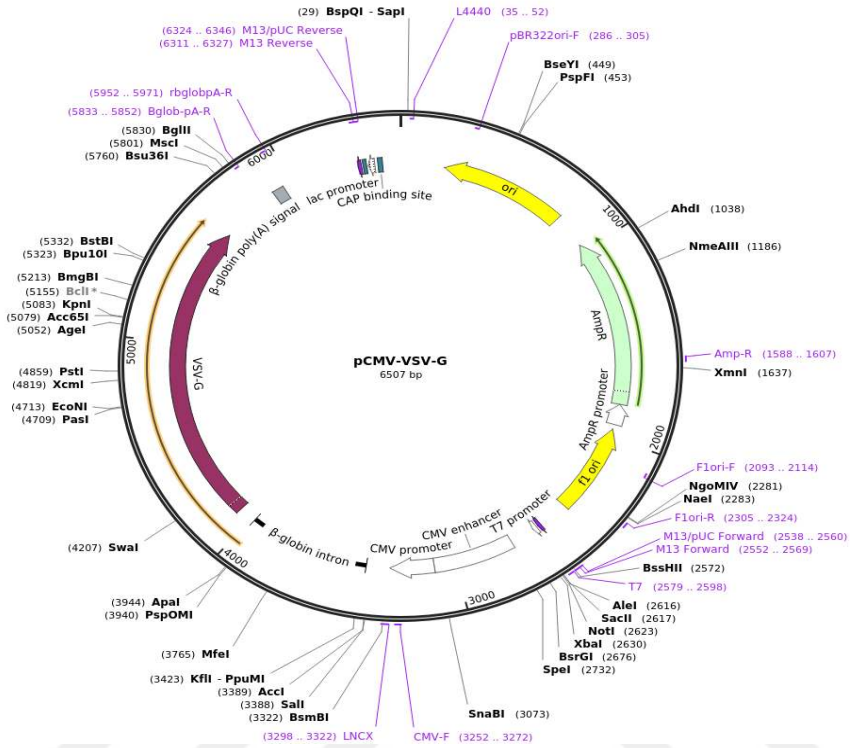

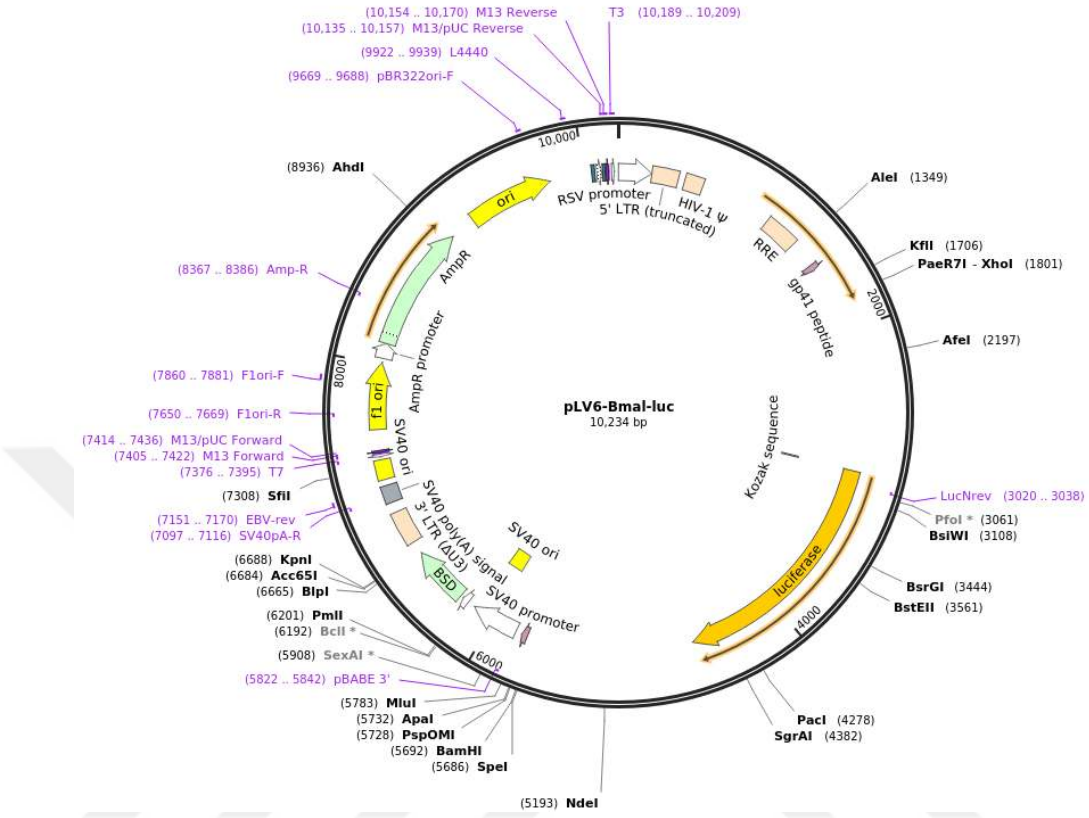

Figure E 1. Maps of expression vectors that used for lentivirus production (from addgene).

BIBLIOGRAPHY

1. Bell. Pedersen, D., et al., Circadian rhythms from multiple oscillators: lessons from diverse organisms. Nature Reviews Genetics, 2005. **6**(7): p. 544. 556.
2. Edgar, R.S., et al., Peroxiredoxins are conserved markers of circadian rhythms. Nature,2012. **485**(7399): p. 459. 464.
3. Johnson, C.H., P.L. Stewart, and M. Egli, The cyanobacterial circadian system: from biophysics to bioevolution. Annual review of biophysics, 2011. 40: p. 143. 167
4. Eelderink. Chen, Z., et al., A circadian clock in Saccharomyces cerevisiae. Proceedings of the National Academy of Sciences, 2010. **107**(5): p. 2043. 2047.
5. Aschoff, J., A survey on biological rhythms, in Biological rhythms. 1981, Springer. p. 3. 10.
6. Foster, R. G. & Roenneberg, T. Human Responses to the Geophysical Daily, Annual and Lunar Cycles. Curr. Biol. **18**, 784–794 (2008).
7. Paul, M.J., I. Zucker, and W.J. Schwartz, Tracking the seasons: the internal calendars of vertebrates. Philosophical Transactions of the Royal Society B: Biological Sciences, 2008.**363**(1490): p. 341. 361.
8. Cohen, S. E., & Golden, S. S. (2015). Circadian rhythms in cyanobacteria. *Microbiology and Molecular Biology Reviews*, **79**(4), 373. 385.
9. Lemmer, B. (2006). The importance of circadian rhythms on drug response in hypertension and coronary heart disease—from mice and man. *Pharmacology & therapeutics*, ***111***(3), 629. 651.
10. Musiek, E. S., Xiong, D. D., & Holtzman, D. M. (2015). Sleep, circadian rhythms, and the pathogenesis of Alzheimer disease. *Experimental & molecular medicine*, **47**(3), e148. e148.
11. Sack, R. L., Brandes, R. W., Kendall, A. R., & Lewy, A. J. (2000). Entrainment of free. running circadian rhythms by melatonin in blind people. *New England Journal of Medicine*, **343**(15), 1070. 1077.
12. Roenneberg, T., & Merrow, M. (2007, January). Entrainment of the human circadian clock. In *Cold Spring Harbor symposia on quantitative biology* (Vol. 72, pp. 293. 299). Cold Spring Harbor Laboratory Press.

13. .Dubowy, C., & Sehgal, A. (2017). Circadian rhythms and sleep in Drosophila melanogaster. *Genetics*, **205**(4), 1373. 1397
14. Wee, R., Castrucci, A. M., Provencio, I., Gan, L., & Van Gelder, R. N. (2002). Loss of photic entrainment and altered free. running circadian rhythms in math5−/− mice. *Journal of Neuroscience*, **22**(23), 10427. 10433.
15. Tahara, Y., & Shibata, S. (2018). Entrainment of the mouse circadian clock: effects of stress, exercise, and nutrition. *Free Radical Biology and Medicine*, **119**, 129. 138.
16. Jennifer, A. M., Caria, B. G. & Joseph, S. T. Central and Peripheral Circadian Clocks in Mammals. Annu. Rev. Neurosci. 445–462 (2012).
17. Buhr, E. D. & Takahashi, J. S. Molecular components of the mammalian circadian clock. Handb. Exp. Pharmacol. **217**, 3–27 (2013).
18. Colwell, C.S., Linking neural activity and molecular oscillations in the SCN. Nature Reviews Neuroscience, 2011. **12**(10): p. 553. 569.
19. Mieda, M., The network mechanism of the central circadian pacemaker of the SCN: Do AVP neurons play a more critical role than expected? Frontiers in neuroscience, 2019. **13**: p. 139.
20. Challet, E., Caldelas, I., Graff, C., & Pévet, P. (2003). Synchronization of the molecular clockwork by light. and food. related cues in mammals.
21. Koronowski, K. B., Kinouchi, K., Welz, P. S., Smith, J. G., Zinna, V. M., Shi, J., ... & Sassone. Corsi, P. (2019). Defining the independence of the liver circadian clock. *Cell*, **177**(6), 1448. 1462.
22. Takahashi, J. S. (2016). Molecular architecture of the circadian clock in mammals. *A time for metabolism and hormones*, **13**. 24.
23. Partch, C. L., Green, C. B., & Takahashi, J. S. (2014). Molecular architecture of the mammalian circadian clock. *Trends in cell biology*, **24**(2), 90. 99.
24. Doruk, Y. U., Yarparvar, D., Akyel, Y. K., Gul, S., Taskin, A. C., Yilmaz, F., ... & Kavakli, I. H. (2020). A CLOCK. binding small molecule disrupts the interaction between CLOCK and BMAL1 and enhances circadian rhythm amplitude. *Journal of Biological Chemistry*, **295**(11), 3518. 3531.

25. Spengler, M. L., Kuropatwinski, K. K., Schumer, M., & Antoch, M. (2009). A serine cluster mediates BMAL1. dependent CLOCK phosphorylation and degradation. *Cell cycle*, **8**(24), 4138. 4146.
26. Shirogane, T., Jin, J., Ang, X. L., & Harper, J. W. (2005). SCFβ. TRCP controls clock. dependent transcription via casein kinase 1. dependent degradation of the mammalian period. 1 (Per1) proteinm. *Journal of Biological Chemistry*, **280**(29), 26863. 26872.
27. Guillaumond, F., Dardente, H., Giguère, V., & Cermakian, N. (2005). Differential control of Bmal1 circadian transcription by REV. ERB and ROR nuclear receptors. *Journal of biological rhythms*, **20**(5), 391. 403.
28. Ukai. Tadenuma, M. et al. Delay in feedback repression by cryptochrome 1 Is required for circadian clock function. Cell **144**, 268–281 (2011).
29. Mehra, A., Baker, C. L., Loros, J. J., & Dunlap, J. C. (2009). Post. translational modifications in circadian rhythms. *Trends in biochemical sciences*, **34**(10), 483. 490.
30. Toh, K. L., Jones, C. R., He, Y., Eide, E. J., Hinz, W. A., Virshup, D. M., ... & Fu, Y. H. (2001). An h Per2 phosphorylation site mutation in familial advanced sleep phase syndrome. *Science*, **291**(5506), 1040. 1043.
31. Vanselow, K., & Kramer, A. (2007, January). Role of phosphorylation in the mammalian circadian clock. In *Cold Spring Harbor symposia on quantitative biology* (Vol. 72, pp. 167. 176). Cold Spring Harbor Laboratory Press.
32. Langmesser, S., Tallone, T., Bordon, A., Rusconi, S., & Albrecht, U. (2008). Interaction of circadian clock proteins PER2 and CRY with BMAL1 and CLOCK. *BMC molecular biology*, ***9***(1), 1. 16.
33. Yoo, S. H., Mohawk, J. A., Siepka, S. M., Shan, Y., Huh, S. K., Hong, H. K., ... & Takahashi, J. S. (2013). Competing E3 ubiquitin ligases govern circadian periodicity by degradation of CRY in nucleus and cytoplasm. *Cell*, ***152***(5), 1091. 1105.
34. Siepka, S. M., Yoo, S. H., Park, J., Song, W., Kumar, V., Hu, Y., ... & Takahashi, J. S. (2007). Circadian mutant Overtime reveals F. box protein FBXL3 regulation of cryptochrome and period gene expression. *Cell*, ***129***(5), 1011. 1023.

35. Hirayama, J., & Sassone. Corsi, P. (2005). Structural and functional features of transcription factors controlling the circadian clock. *Current opinion in genetics & development*, ***15***(5), 548. 556.
36. Lee, Y., Chen, R., Lee, H. M. & Lee, C. Stoichiometric relationship among clock proteins determines robustness of circadian rhythms. J. Biol. Chem. **286**, 7033–7042 (2011).
37. Kondratov, R. V., Chernov, M. V., Kondratova, A. A., Gorbacheva, V. Y., Gudkov, A. V., & Antoch, M. P. (2003). BMAL1. dependent circadian oscillation of nuclear CLOCK: posttranslational events induced by dimerization of transcriptional activators of the mammalian clock system. *Genes & development*, ***17***(15), 1921. 1932.
38. Miki, T., Xu, Z., Chen-Goodspeed, M., Liu, M., Van Oort-Jansen, A., Rea, M. A., ... & Chang, K. S. (2012). PML regulates PER2 nuclear localization and circadian function. *The EMBO journal*, ***31***(6), 1427. 1439.
39. Cal-Kayitmazbatir, S., Kulkoyluoglu-Cotul, E., Growe, J., Selby, C. P., Rhoades, S. D., Malik, D., ... & Kavakli, I. H. (2021). CRY1-CBS binding regulates circadian clock function and metabolism. *The FEBS journal*, ***288***(2), 614. 639.
40. Zhang, E. E. et al. A Genome. wide RNAi Screen for Modifiers of the Circadian Clock in Human Cells. Cell **139**, 199–210 (2009).
41. Kavakli, I. H., Gul, S., & Turkay, M. (2022). Identification of novel small molecules targeting core clock proteins to regulate circadian rhythm. *Current Opinion in Chemical Engineering*, ***35***, 100730.
42. Gul, S., Rahim, F., Isin, S., Yilmaz, F., Ozturk, N., Turkay, M., & Kavakli, I. H. (2021). Structure. based design and classifications of small molecules regulating the circadian rhythm period. *Scientific reports*, ***11***(1), 1. 15.
43. Campisi, J. (2013). Aging, cellular senescence, and cancer. *Annual review of physiology*, ***75***, 685.
44. Ubbink, J. B., Vermaak, W. H., van Der Merwe, A., & Becker, P. J. (1992). The effect of blood sample aging and food consumption on plasma total homocysteine levels. *Clinica chimica acta*, ***207***(1. 2), 119. 128.

45. Harrison, D. E., & Archer, J. R. (1987). Genetic differences in effects of food restriction on aging in mice. *The Journal of nutrition*, ***117***(2), 376. 382.
46. Harrison, D. E., Archer, J. R., & Astle, C. M. (1984). Effects of food restriction on aging: separation of food intake and adiposity. *Proceedings of the National Academy of Sciences*, ***81***(6), 1835. 1838.
47. Muñoz. Espín, D., & Serrano, M. (2014). Cellular senescence: from physiology to pathology. *Nature reviews Molecular cell biology*, ***15***(7), 482. 496.
48. Tominaga, K., Olgun, A., Smith, J. R., & Pereira. Smith, O. M. (2002). Genetics of cellular senescence. *Mechanisms of ageing and development*, ***123***(8), 927. 936.
49. Nakagawa, H., Sasagawa, S., & Itoh, K. (2018). Sodium butyrate induces senescence and inhibits the invasiveness of glioblastoma cells. *Oncology letters*, ***15***(2), 1495. 1502.
50. Furukawa, M., Mimura, Y., Tao, H., Mimura, Y., & Okabe, K. (2016). 5. aza. 2'. Deoxycytidine induces cellular senescence in non. small cell lung cancer. *Cancer Research*, ***76***(14_Supplement), 2842. 2842.
51. Rufini, A., Tucci, P., Celardo, I., & Melino, G. (2013). Senescence and aging: the critical roles of p53. *Oncogene*, ***32***(43), 5129-5143.
52. Effros, R. B., & Walford, R. L. (1984). T cell cultures and the Hayflick limit. *Human immunology*, ***9***(1), 49. 65.
53. Dodig, S., Čepelak, I., & Pavić, I. (2019). Hallmarks of senescence and aging. *Biochemia medica*, ***29***(3), 483. 497.
54. Herbig, U., Ferreira, M., Condel, L., Carey, D., & Sedivy, J. M. (2006). Cellular senescence in aging primates. *Science*, ***311***(5765), 1257-1257.
55. Fathi, E., Charoudeh, H. N., Sanaat, Z., & Farahzadi, R. (2019). Telomere shortening as a hallmark of stem cell senescence. *Stem cell investigation*, ***6***.
56. Derevyanko, A., Whittemore, K., Schneider, R. P., Jiménez, V., Bosch, F., & Blasco, M. A. (2017). Gene therapy with the TRF 1 telomere gene rescues decreased TRF 1 levels with aging and prolongs mouse health span. *Aging cell*, ***16***(6), 1353. 1368.
57. Calado, R. T., & Young, N. S. (2009). Telomere diseases. *New England Journal of Medicine*, ***361***(24), 2353. 2365.

58. Richards, L. A., Kumari, A., Knezevic, K., Thoms, J. A., von Jonquieres, G., Napier, C. E., ... & MacKenzie, K. L. (2020). DKC1 is a transcriptional target of GATA1 and drives upregulation of telomerase activity in normal human erythroblasts. *Haematologica*, ***105***(6), 1517.
59. Blasco, M. A. (2007). Telomere length, stem cells and aging. *Nature chemical biology*, ***3***(10), 640. 649.
60. Nakamura, T. J., Nakamura, W., Tokuda, I. T., Ishikawa, T., Kudo, T., Colwell, C. S., & Block, G. D. (2015). Age. related changes in the circadian system unmasked by constant conditions. *Eneuro*, ***2***(4).
61. Yamazaki, S., Straume, M., Tei, H., Sakaki, Y., Menaker, M., & Block, G. D. (2002). Effects of aging on central and peripheral mammalian clocks. *Proceedings of the National Academy of Sciences*, ***99***(16), 10801. 10806.
62. Nakahata, Y., Kaluzova, M., Grimaldi, B., Sahar, S., Hirayama, J., Chen, D., ... & Sassone. Corsi, P. (2008). The NAD+. dependent deacetylase SIRT1 modulates CLOCK. mediated chromatin remodeling and circadian control. *Cell*, ***134***(2), 329. 340.
63. Masri, S., Rigor, P., Cervantes, M., Ceglia, N., Sebastian, C., Xiao, C., ... & Sassone. Corsi, P. (2014). Partitioning circadian transcription by SIRT6 leads to segregated control of cellular metabolism. *Cell*, ***158***(3), 659. 672.
64. Ahmed, R., Reza, H. M., Shinohara, K., & Nakahata, Y. (2022). Cellular senescence and its impact on the circadian clock. *The Journal of Biochemistry*, ***171***(5), 493. 500.
65. Rutter, J., Reick, M., Wu, L.C., and McKnight, S.L. (2001) Regulation of clock and NPAS2 DNA binding by the redox state of NAD cofactors. Science **293**, 510–514.
66. Jee, H.U., Yang, S., Yamazaki, S., Kang, H., Viollet, B.,Foretz, M., and Chung, J.H. (2007) Activation of 5 # . AMP. activated kinase with diabetes drug metformin induces casein kinase Iε (CKIε). dependent degradation of clock protein mPer2. J. Biol. Chem. **282**, 20794–20798.
67. Dudek, M., Yang, N., Ruckshanthi, J. P., Williams, J., Borysiewicz, E., Wang, P., ... & Meng, Q. J. (2017). The intervertebral disc contains intrinsic circadian clocks that are regulated by age and cytokines and linked to degeneration. *Annals of the rheumatic diseases*, ***76***(3), 576. 584.

68. Hirota T, Lee JW, St John PC, Sawa M, Iwaisako K, Noguchi T, Pongsawakul PY, Sonntag T, Welsh DK, Brenner DA et al.: Identification of small molecule activators of cryptochrome. Science 2012, 3**37**:1094-1097
69. He B, Nohara K, Park N, Park Y-S, Guillory B, Zhao Z, Garcia Jose M, Koike N, Lee Cheng C, Takahashi Joseph S et al.: The small molecule nobiletin targets the molecular oscillator to enhance circadian rhythms and protect against metabolic syndrome. Cell Metab 2016, **23**:610-621.
70. Gul S, Akyel YK, Gul ZM, Isin S, Korkmaz T, Selvi S, Danis I, Ipek OS, Aygenli F, Taskin AC et al.: Discovery of a small molecule that selectively destabilizes cryptochrome 1 and enhances life span in p53 knockout mice. BioRxiv 2021. 2021.2007.2021.453206.
71. Miller S, Aikawa Y, Sugiyama A, Nagai Y, Hara A, Oshima T, Amaike K, Kay SA, Itami K, Hirota T: An isoform-selective modulator of cryptochrome 1 regulates circadian rhythms in mammals. Cell Chem Biol 2020, **27**:1192-1198.e5.
72. Oshima T, Yamanaka I, Kumar A, Yamaguchi J, NishiwakiOhkawa T, Muto K, Kawamura R, Hirota T, Yagita K, Irle S et al.: CH activation generates period-shortening molecules that target cryptochrome in the mammalian circadian clock. Angew Chem Int Ed Engl 2015, **54**:7193-7197.
73. Huschtscha, L. I., & Holliday, R. (1983). Limited and unlimited growth of SV40-transformed cells from human diploid MRC-5 fibroblasts. *Journal of cell science*, ***63***(1), 77-99.
74. Merker, K., Sitte, N., & Grune, T. (2000). Hydrogen peroxide-mediated protein oxidation in young and old human MRC-5 fibroblasts. *Archives of biochemistry and biophysics*, ***375***(1), 50-54.
75. Hodge, R. A., & Perkins, R. M. (1989). Mode of action of 9-(4-hydroxy-3-hydroxymethylbut-1-yl) guanine (BRL 39123) against herpes simplex virus in MRC-5 cells. *Antimicrobial Agents and Chemotherapy*, ***33***(2), 223-229.
76. Zielinski, T., Moore, A. M., Troup, E., Halliday, K. J., & Millar, A. J. (2014). Strengths and limitations of period estimation methods for circadian data. *PloS one*, ***9***(5), e96462.

77. Gentleman, R. C., Carey, V. J., Bates, D. M., Bolstad, B., Dettling, M., Dudoit, S., ... & Zhang, J. (2004). Bioconductor: open software development for computational biology and bioinformatics. *Genome biology*, ***5***(10), 1-16.
78. Dobin, A., Davis, C. A., Schlesinger, F., Drenkow, J., Zaleski, C., Jha, S., ... & Gingeras, T. R. (2013). STAR: ultrafast universal RNA-seq aligner. *Bioinformatics*, ***29***(1), 15-21.
79. Wu, G., Anafi, R. C., Hughes, M. E., Kornacker, K., & Hogenesch, J. B. (2016). MetaCycle: an integrated R package to evaluate periodicity in large scale data. *Bioinformatics*, ***32***(21), 3351-3353.
80. Zhang, R., et al., A circadian gene expression atlas in mammals: implications for biology and medicine. Proceedings of the National Academy of Sciences, 2014. **111**(45): p.16219-16224.
81. Kanehisa, M. (2002, January). The KEGG database. In *Novartis foundation symposium* (pp. 91-100). Chichester; New York; John Wiley; 1999.
82. Kanehisa, M., Furumichi, M., Tanabe, M., Sato, Y., & Morishima, K. (2017). KEGG: new perspectives on genomes, pathways, diseases and drugs. *Nucleic acids research*, ***45***(D1), D353-D361.
83. Wolff, C. A., Gutierrez-Monreal, M. A., Meng, L., Zhang, X., Douma, L. G., Costello, H. M., ... & Esser, K. A. (2022). Defining the age-dependent and tissue-specific circadian transcriptome in male mice. *bioRxiv*.
84. Kirkland, J. L., & Tchkonia, T. (2020). Senolytic drugs: from discovery to translation. *Journal of internal medicine*, ***288***(5), 518-536.
85. Niedernhofer, L. J., & Robbins, P. D. (2018). Senotherapeutics for healthy ageing. *Nature Reviews Drug Discovery*, ***17***(5), 377-377.
86. Fonseca Costa, S. S., & Ripperger, J. A. (2015). Impact of the circadian clock on the aging process. *Frontiers in neurology*, ***6***, 43.
87. Kondratov, R. V., Kondratova, A. A., Gorbacheva, V. Y., Vykhovanets, O. V., & Antoch, M. P. (2006). Early aging and age-related pathologies in mice deficient in BMAL1, the core componentof the circadian clock. *Genes & development*, ***20***(14), 1868-1873.

88. Wyse, C. A., & Coogan, A. N. (2010). Impact of aging on diurnal expression patterns of CLOCK and BMAL1 in the mouse brain. *Brain research*, ***1337***, 21-31.
89. Macias, E., Kim, Y., Miliani de Marval, P. L., Klein-Szanto, A., & Rodriguez-Puebla, M. L. (2007). Cdk2 deficiency decreases ras/CDK4-dependent malignant progression, but not myc-induced tumorigenesis. *Cancer research*, ***67***(20), 9713-9720.
90. Gopinathan, L., Tan, S. L. W., Padmakumar, V. C., Coppola, V., Tessarollo, L., & Kaldis, P. (2014). Loss of Cdk2 and Cyclin A2 Impairs Cell Proliferation and TumorigenesisDelayed Tumorigenesis in the Absence of Cyclin A2. *Cancer research*, ***74***(14), 3870-3879.
91. Hydbring, P., & Larsson, L. G. (2010). Cdk2: a key regulator of the senescence control function of Myc. *Aging (Albany NY)*, ***2***(4), 244.
92. Jurk D, Wilson C, Passos JF, Oakley F, Correia-Melo C, Greaves L, Saretzki G, Fox C, Lawless C, Anderson R *et al*. (2014) Chronic inflammation induces telomere dysfunction and accelerates ageing in mice. *Nat Commun* **2**, 4172.
93. Bernal M, Wahlstrom JS, Crawley CD, Cahill KE, Pytel P, Liang H, Kang S, Weichselbaum RR & Yamini B (2014) Loss of Nfkb1 leads to early onset aging. *Aging (Albany NY)* **6**, 931–942.
94. Yamini, B. (2015). Nfkb1/p50 and mammalian aging. *Oncotarget*, *6*(6), 3471.
95. Ortega-Molina, A., & Serrano, M. (2013). PTEN in cancer, metabolism, and aging. *Trends in Endocrinology & Metabolism*, ***24***(4), 184-189.
96. Kitagishi, Y., & Matsuda, S. (2013). Redox regulation of tumor suppressor PTEN in cancer and aging. *International journal of molecular medicine*, ***31***(3), 511-515.
97. Pizarro, A., Hayer, K., Lahens, N. F., & Hogenesch, J. B. (2012). CircaDB: a database of mammalian circadian gene expression profiles. *Nucleic acids research*, ***41***(D1), D1009-D1013.
98. Chen, W. D., Wen, M. S., Shie, S. S., Lo, Y. L., Wo, H. T., Wang, C. C., ... & Wang, C. Y. (2014). The circadian rhythm controls telomeres and telomerase activity. *Biochemical and biophysical research communications*, ***451***(3), 408-414.

99. Jiang, X. R., Jimenez, G., Chang, E., Frolkis, M., Kusler, B., Sage, M., ... & Chiu, C. P. (1999). Telomerase expression in human somatic cells does not induce changes associated with a transformed phenotype. *Nature genetics*, ***21***(1), 111-114.

100. Guo, B., Yang, N., Borysiewicz, E., Dudek, M., Williams, J. L., Li, J., ... & Meng, nQ. J. (2015). Catabolic cytokines disrupt the circadian clock and the expression of clock. controlled genes in cartilage via an NFκB. dependent pathway. *Osteoarthritis and cartilage*, *23*(11), 1981. 1988.

101. Sidler, C., Kovalchuk, O., & Kovalchuk, I. (2017). Epigenetic regulation of cellular senescence and aging. *Frontiers in genetics*, ***8***, 138.

102. Cheng, L. Q., Zhang, Z. Q., Chen, H. Z., & Liu, D. P. (2017). Epigenetic regulation in cell senescence. *Journal of Molecular Medicine*, ***95***(12), 1257-1268.

103. Levine, M. E. (2020). Assessment of epigenetic clocks as biomarkers of aging in basic and population research. *The Journals of Gerontology: Series A*, ***75***(3), 463-465.

104. Ray, S., Lach, R., Heesom, K. J., Valekunja, U. K., Encheva, V., Snijders, A. P., & Reddy, A. B. (2019). Phenotypic proteomic profiling identifies a landscape of targets for circadian clock–modulating compounds. *Life science alliance*, ***2***(6).

105. Yalçin, M., El-Athman, R., Ouk, K., Priller, J., & Relógio, A. (2020). Analysis of the circadian regulation of cancer hallmarks by a cross-platform study of colorectal cancer time-series data reveals an association with genes involved in Huntington's disease. *Cancers*, ***12***(4), 963.

106. Matsumoto, C. S., Almeida, L. O., Guimarães, D. M., Martins, M. D., Papagerakis, P., Papagerakis, S., ... & Squarize, C. H. (2016). PI3K-PTEN dysregulation leads to mTOR-driven upregulation of the core clock gene BMAL1 in normal and malignant epithelial cells. *Oncotarget*, ***7***(27), 42393.

107. Alibhai, F. J., LaMarre, J., Reitz, C. J., Tsimakouridze, E. V., Kroetsch, J. T., Bolz, S.S., & Martino, T. A. (2017). Disrupting the key circadian regulator CLOCK leads to age-dependent cardiovascular disease. *Journal of molecular and cellular cardiology*, ***105***, 24-37.

108. Kolde, R., & Kolde, M. R. (2018). Package 'pheatmap'. *R Package*, ***1***.

109. Guo, B., Yang, N., Borysiewicz, E., Dudek, M., Williams, J. L., Li, J., ... & Meng,

Q. J. (2015). Catabolic cytokines disrupt the circadian clock and the expression of clock. controlled genes in cartilage via an NFκB. dependent pathway. *Osteoarthritis and cartilage*, ***23***(11), 1981. 1988.

110. Debacq-Chainiaux, F., Erusalimsky, J. D., Campisi, J., & Toussaint, O. (2009). Protocols to detect senescence-associated beta-galactosidase (SA-βgal) activity, a biomarker of senescent cells in culture and in vivo. Nature protocols, 4(12), 1798-1806.